

# **Meteorological constraints on oceanic halocarbons above the Peruvian Upwelling**

**S. Fuhlbrügge<sup>1</sup>, B. Quack<sup>1</sup>, E. Atlas<sup>2</sup>, A. Fiehn<sup>1</sup>, H. Hepach<sup>1</sup>, K. Krüger<sup>3</sup>**

[1] GEOMAR | Helmholtz Centre for Ocean Research Kiel

[2] Rosenstiel School for Marine and Atmospheric Sciences, Miami, Florida

[3] University of Oslo, Oslo, Norway

Correspondence to: K. Krüger ([kirstin.krueger@geo.uio.no](mailto:kirstin.krueger@geo.uio.no))

## ***Response to Referee #1***

### **General Comments:**

*Referee #1:*

*This paper presents a new dataset of halocarbon observations along the Peruvian coast and the upwelling region nearby. The observations add to a scant dataset of halocarbons and helps in completing the global picture in addition to explaining some local differences. Additionally the fluxes calculated will undoubtedly be useful to modelling groups, which have been struggling with getting a complete emission inventory for several of the compounds measured here. I recommend the manuscript is published in ACP, after the authors have addressed a few points that are detailed below.*

Author's response:

We first would like to thank the reviewer 1 for reviewing the manuscript and for the overall positive evaluation of the paper, which she/he describes as helpful in completing the global picture of halocarbons observations and useful to modelling groups with getting a complete emission inventory. Below you find our point-by-point answers to your comments (*highlighted in italic*).

### **Major comments:**

*1) Although the authors mention that the fluxes are different to the other locations, such as the Mauritanian upwelling, there isn't much discussion about the reasons for this. One reason that is mentioned is the difference in the wind speed and the ocean atmosphere gradient. Why do the authors rule out biological processes? Maybe some light can be shed on this using ocean colour data, and/or phytoplankton speciation data.*

We agree with the reviewer that biological processes in the oceans often play an important role for the concentration distribution of brominated and iodinated VSLs, and therefore also for their concentration gradient, being a major driver for their sea-to-air fluxes. The analysis of biological parameters was not part and scope of this manuscript. The relation of pigments, phytoplankton groups, dissolved organic matter and bacteria to the halogenated VSLs are covered in an accompanying manuscript by Hepach et al. (submitted January 2016). For further discussion on the distribution of the oceanic halocarbons and biological processes, see Hepach et al. (2016, submitted).

Fluxes for CH<sub>3</sub>I were much higher in the Peruvian upwelling (M91 cruise) than in the Mauritanian upwelling (DRIVE cruise), because of the higher oceanic concentrations. This can be probably linked to biological production, as high correlations with Chl *a* and diatoms were found, in contrast to lower concentrations of CH<sub>3</sub>I in surface waters of the Mauritanian upwelling during June 2010, linked to photochemical production (Hepach et al., 2014). Production of bromocarbons was seemingly much lower in the Peruvian upwelling than in the Mauritanian upwelling, although biological parameters as total chlorophyll concentrations were similar in both regions. As iodinated compounds were much higher in the Peruvian upwelling, different production mechanisms for bromocarbons and iodocarbons can be hypothesized. Ambient conditions and different phytoplankton species in the Peruvian upwelling may have favoured production of iodocarbons rather than of bromocarbons during the time (December 2012) and in the region of the M91 cruise. The lower concentrations of bromocarbons and lower wind speeds both reduce the sea to air fluxes via both the concentration gradient and  $k_w$  leading to much lower sea-to-air fluxes in the Peruvian upwelling than in the Mauritanian upwelling.

*2) The authors have mentioned that the transport paths might explain the elevated IO observed by Schönhardt et al. However, the transport paths take about 5-8 days, which is much longer than the lifetime of CH<sub>3</sub>I and hence its contribution should not be as high. Very low concentrations of IO have also been observed at the Galapagos Islands, although higher CH<sub>3</sub>I was observed. Closer analysis of the CH<sub>3</sub>I data had indicated a local source rather than transport from the Peruvian upwelling region (Gomez-Martin et al., 2013).*

We agree with the reviewer that the lifetime of methyl iodide is too short to be transported from the cruise track towards the equatorial East Pacific and Galapagos Islands before being degraded and that therefore local sources appear likely. However, the observed elevated methyl iodide mixing ratios during the cruise could explain part of the elevated IO above the Peruvian upwelling (Hepach et al., 2016, submitted) as was also observed by Schönhardt et al. (2008). We clarified this in the manuscript now by writing:

“A contribution of oceanic emissions from the Peruvian Upwelling to the free troposphere is only achieved in the inner tropics after a transport time of 5 – 8 days, where the VLSL abundances are transported into higher altitudes. Since the lifetime of methyl iodide is only 4 days in the MABL a significant contribution of methyl iodide from the Peruvian upwelling to

the observations made by Yokouchi et al. (2008) at San Cristobal, Galapagos is not to be expected. However, it can partly explain the elevated IO observed above the Peruvian upwelling (Hepach et al., 2016, submitted; Schönhardt et al., 2008).”

*3) The quantitative analysis of the dependence of the flux is only limited to doing Spearman correlations and the dependence between boundary layer and concentrations is shown in a figure. Considering the low spearman's coefficients and high P values (0.05), I suggest that the authors conduct a two dimensional principal component analysis of the dataset considering all the different parameters measured. This will help in better understanding the major driving factors, rather than doing simple correlation coefficient calculations, especially, which do not have a high significance (<0.01). Several of the measured parameters could correlate, but that does not necessarily show any causality as evidenced in table 3.*

According to the reviewers suggestion we conducted a two-dimensional principle component analysis (PCA). However, a PCA transforms a number of correlated variables into a number of uncorrelated variables. Thus considering all the different parameters measured with their relatively low correlation coefficients a PCA in this case appears unnecessary. Nevertheless we performed a PCA on the relative humidity, wind speed, sea surface temperature (SST), surface air temperature (SAT), MABL height and atmospheric mixing ratios of  $\text{CHBr}_3$ ,  $\text{CH}_2\text{Br}_2$  and  $\text{CH}_3\text{I}$ , which are correlated to each other. The according ‘loadings plot’ (Figure A) reveals two cluster. The first cluster includes the atmospheric VSLs mixing ratios of  $\text{CH}_3\text{I}$ ,  $\text{CHBr}_3$  and  $\text{CH}_2\text{Br}_2$  and the relative humidity. The second cluster includes the MABL height, SST and SAT. These two clusters are forming, since the variables in one cluster are negatively correlated to the variables in the opposite cluster. However, the wind speed with its low spearman correlation coefficients reveals to be no driving factor of the remaining variables. We will add this to the manuscript:

“A principle component analysis of the parameters in Table 3 furthermore revealed a distinct relation between SAT, SST, MABL height, relative humidity and atmospheric mixing ratios of  $\text{CHBr}_3$  and  $\text{CH}_2\text{Br}_2$  (not shown here).”

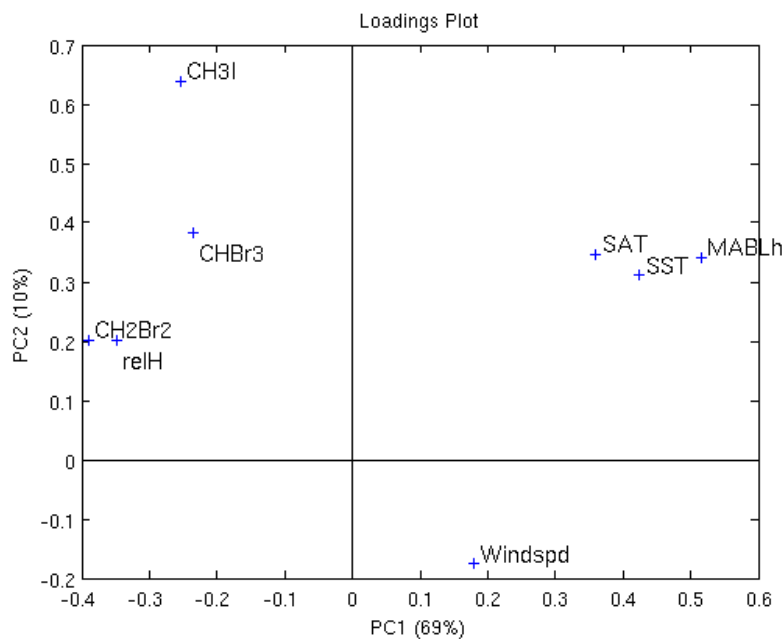


Figure A: Loadings plot of 1<sup>st</sup> and 2<sup>nd</sup> principle component (PC). Two clusters form: 1. CHBr<sub>3</sub>, CH<sub>2</sub>Br<sub>2</sub> and relative humidity (relH). 2. SAT, SST and MABL height (MABLh).

**Minor comments:**

1) Please mention the P values for the correlation coefficients in section 3.5

Done.: “Indeed, we also find significant ( $p < 0.05$ ) high correlations [...]”

2) The Martin et al 2013 reference should be Gomez-Martin et al, 2013

Done.

References

Hepach, H., Quack, B., Ziska, F., Fuhlbrügge, S., Atlas, E., Krüger, K., Peeken, I., and Wallace, D. W. R.: Drivers of diel and regional variations of halocarbon emissions from the tropical North East Atlantic, *Atmos. Chem. Phys.*, 14, 10.5194/acp-14-1255-2014, 2014.

Hepach, H., Quack, B., Tegtmeier, S., Engel, A., Bracher, A., Fuhlbrügge, S., L., G., Atlas, E., Lampel, J., Frieß, U., and Krüger, K.: Biogenic halocarbons from the Peruvian upwelling region as tropospheric halogen source, to be submitted, 2016.

Schönhardt, A., Richter, A., Wittrock, F., Kirk, H., Oetjen, H., Roscoe, H., and Burrows, J.: Observations of iodine monoxide columns from satellite, *Atmospheric Chemistry and Physics*, 8, 637-653, 10.5194/acp-8-637-2008, 2008.

Yokouchi, Y., Osada, K., Wada, M., Hasebe, F., Agama, M., Murakami, R., Mukai, H., Nojiri, Y., Inuzuka, Y., Toom-Sauntry, D., and Fraser, P.: Global distribution and seasonal concentration change of methyl iodide in the atmosphere, *Journal of Geophysical Research-Atmospheres*, 113, 10.1029/2008JD009861, 2008.

## ***Response to Referee #2***

We would like to thank reviewer 2 for reviewing the manuscript. Below you find our point-by-point answers to your comments (*highlighted in italic*).

### **General Comments:**

*Referee #2:*

*The manuscript is reasonably well written but at times a little difficult to follow, owing in part to acronyms and repeated recitation of numbers, but also to text that seems to ramble without a clear focus in some places.*

Author's response:

We have carefully revised the text taking your suggestions into account. Thus, we changed in particular Sections 3.2-3.5, 4 and 5, reduced the acronyms and repeated numbers, which are already listed in the tables. Further details can be found in our answers to your specific comments below.

*The sampling approach appears sound, the data look to be good, and the approach is interesting. I'm wondering, however, if the authors are not letting the "trees get in the way of seeing the forest", in that in some places the detail is killing the main message.*

*Using a largely meteorological approach, the authors make the case that the ocean makes only a small contribution to the amount of gas in the boundary layer immediately above it. While that may be true for any of the 400 m<sup>2</sup> boxes they use, I'm not so certain it is true for Peruvian upwelling altogether. At least, that has not been made clear to me. The point is made that most of the halocarbons over a given area are advected in, but it belies the possibility (probability?) that any elevation of concentration in a particular box coming from upwind portions of the upwelling zone contains air that has already been impacted by oceanic emissions. One could walk away from this paper thinking that the emissions of short lived halocarbons in upwelling regions like Peru are not that significant when, based on comparison with boundary layer burdens over the open ocean, it seems that they are. This is not to say that the analysis in this paper is not useful, but it does need to be put in perspective. The authors also need to discuss the tenuous nature of their assumption of steady state in a dynamic boundary layer and its implications to their conclusions.*

We agree with the reviewer that the paper should avoid the impression, that the emissions of short lived halocarbons in upwelling regions like Peru are not that significant when, based on comparison with boundary layer burdens over the open ocean, it seems that they are. We also agree with the reviewer that the boundary layer burdens over the upwelling are much more significant than over the open ocean which is generally due to elevated oceanic concentrations and emissions in conjunction with stable layers in the atmosphere above upwelling regions. However during M91, the oceanic emissions, which were calculated along the cruise, are indeed generally not sufficient to explain the observed elevated atmospheric mixing ratios in the MABL, which therefore need advection. We add a more detailed description of the observed atmospheric phenomena and methodological constraints in the answer to the reviewer (below) and in the manuscript and therewith hope to better clarify our observations and interpretations of them.

Figure 3e of the manuscript shows that the observed atmospheric mixing ratios of all compounds show background concentrations of around 0.6 ppt for  $\text{CH}_3\text{I}$ , 1 ppt for  $\text{CH}_2\text{Br}_2$  and 2 ppt for  $\text{CHBr}_3$  along the whole cruise with varying elevations in the upwelling regions. The mixing ratios for  $\text{CH}_2\text{Br}_2$  and  $\text{CHBr}_3$  generally double (increase by 1 or 2 ppt above the direct Peruvian upwelling), while  $\text{CH}_3\text{I}$  is 3 to 4 times higher. The observed mean fluxes during the cruise can explain around 0.6 ppt for methyl iodide for an average MABL height of 300 m using a mean residence time of 7hr (derived from our FLEXPART trajectories), and 1.2 ppt under the average trade wind inversion of 1000 m using a mean residence time of 48 hrs. For the low fluxes of  $\text{CH}_2\text{Br}_2$  and  $\text{CHBr}_3$  the contribution to the MABL box is only between 0.1 and 0.3 ppt. Thus, while  $\text{CH}_3\text{I}$ -emissions can explain the local background,  $\text{CH}_2\text{Br}_2$  and  $\text{CHBr}_3$  fluxes cannot. Therefore, we believe that the bromocarbon background mixing ratios of 1 to 2 ppt in the MABL have to be advected, with the southerly low level flow parallel to the coast and below the trade inversion before the air masses reach the well-defined isolated MABL above the Peruvian upwelling. We also agree that a different emissions scenario before the cruise and in waters close to the cruise track may partly explain the discrepancy. However, we believe that during the time of the cruise a representative area of the Peruvian upwelling from 6 °S to 16 °S and 10 nm to 90 nm away from the coast was investigated. Surprisingly high sea surface concentrations and emissions in the upwelling waters different to those measured during the cruise appear unlikely to us. Next to this we even derive from observations that the ocean was mainly a sink for  $\text{CHBr}_3$  between Dec 21 and 25. Also possible elevated emissions from coastal sources, not measured during the cruise, likely add to the atmospheric mixing ratios. Indeed elevated coastal emissions could

explain the threefold increase of  $\text{CHBr}_3$  atmospheric mixing ratios on December 25 with SE wind from the coast (Figure 3), in contrast to Dec 17 when the ship passed the same coastal position but revealing lower VMR and a southern flow. Additionally, direct above the upwelling regions the MABL can be as low as 10 m and shows a mean of 100 m (Figure 4c). Thus local emissions mix into a much lower boundary. As an example an emission of  $1000 \text{ pmol m}^{-2} \text{ hr}^{-1}$  explain an atmospheric mixing ratio increase of 1.75 ppt during a residence time of 7 hr and a MABL height of 100 m. These relatively high emissions have occasionally been observed during the cruise for methyl iodide and the resulting increase in mixing ratios can be even higher in lower MABLs. These high emissions have however barely been observed for  $\text{CHBr}_3$  and  $\text{CH}_2\text{Br}_2$  and are also unlikely due to the low water concentrations and low wind speeds observed during the cruise. Thus, we conclude that coastal contributions with highly elevated emissions of e.g. macro algae are very likely as additional sources for the bromocarbons.

Overall we conclude that the variable and elevated atmospheric mixing ratios observed above the East Pacific and the Peruvian upwelling region, including both open and coastal ocean, can be explained by a mix of oceanic sources and atmospheric phenomena.

In addition the mechanism and concept of the air-sea exchange contribution could be different in the coastal upwelling, e.g. the stable low MABL, which leads to suppressed vertical mixing of surface air, could lead to a gradient of the near surface VSLs with height. Thus, the surface VSLs observations may therefore only be representative for the low and not for the entire MABL column. Next to these considerations, the very low MABL events above the cold, near-coastal waters, which theoretically increase the oceanic contribution to the atmosphere could often not be taken into account in the source/loss estimates due to the low resolved topography in ERA-Interim affecting the trajectory modelling (see manuscript: Section 2.5, Figure 3d). Finally, we also agree that our steady state assumption for the individual box model calculations in the MABL could also be affected by dynamical meteorological fluctuations (e.g. wind and MABL changes). These fluctuations were however quite rare during the time of our ship cruise. Overall, we think that follow-up studies are needed for the East Pacific regime including more marine observations also resolving MABL gradients and high resolution transport modelling including the coast lines.

We add this discussion to Section 4 and an outlook in Section 5 to better address these issues and to put our Peruvian Upwelling analysis in a broader perspective.

*Finally, while the authors do address the uncertainties of ocean concentrations and atmospheric mixing ratios, I'm concerned about the uncertainties introduced by the modeled components, e.g., advection, degradation, air-sea exchange, and how they might impact the authors' conclusions. These seem to be ignored. The authors should at least discuss this, if not address it quantitatively.*

We agree and will include a discussion of the method uncertainties into the existing discussion in Section 4:

“Uncertainties may result from the applied method, which accounts for a 400 m<sup>2</sup> box around a measurement point assuming steady state. The cruise track covered a significantly large area of the Peruvian Upwelling between 5° S and 16° S and higher elevated seas surface concentrations and emissions are not to be expected during these rather stable meteorological conditions. Additional uncertainties in our source-loss estimate may arise from deficiencies in the meteorological input fields from ERA-Interim reanalysis as well as from the air mass transport simulated by FLEXPART. Both could lead to either a shorter or longer residence time of the surface air masses within the MABL or below the trade inversion and thus influence the COL term. In particular very close to the coast, where the source-loss estimate could not be applied due to the trajectory analysis gaps (Section 2.5), the ODRs of the compounds might be different. Here potential high coastal emissions in combination with stable atmospheric stratification leading to slow vertical transport into the free troposphere, could significantly increase the oceanic contribution to the MABL and to the atmosphere below the trade inversion and explain the elevated atmospheric mixing ratios. In addition, different parameterizations for the wind-based transfer coefficient  $k_w$ , as discussed in Lennartz et al. (2015) and Fuhlbrügge et al (2015) in more detail, can impact the air-sea gas exchange and thus the ODRs. Applying the  $k_w$  parameterizations of Liss and Merlivat (1986) as well as Wanninkhof and McGillis (1999) lead both to mean ODRs in the MABL of 0.02 (bromoform), 0.07 (dibromomethane) and 0.21 (methyl iodide) and below the trade inversion of 0.08 / 0.08 (bromoform), 0.25 / 0.26 (dibromomethane) and 0.69 / 0.75 (methyl iodide) and thus an even lower oceanic contribution to the atmosphere in this region. Further uncertainties may arise from variations of the MABL VSLs lifetimes and thus the chemical degradation of the compounds we use in this study. This would affect the computed advection (ADR) and not the oceanic contribution.”

**Specific Comments:**

1. The repeated use of similar acronyms requires that the reader keep looking back at the text. This could be helped considerably with a labeled diagram of the boundary layer box and its fluxes over the 400 m<sup>2</sup> ocean surface.

We agree and add this diagram of the processes into the manuscript:

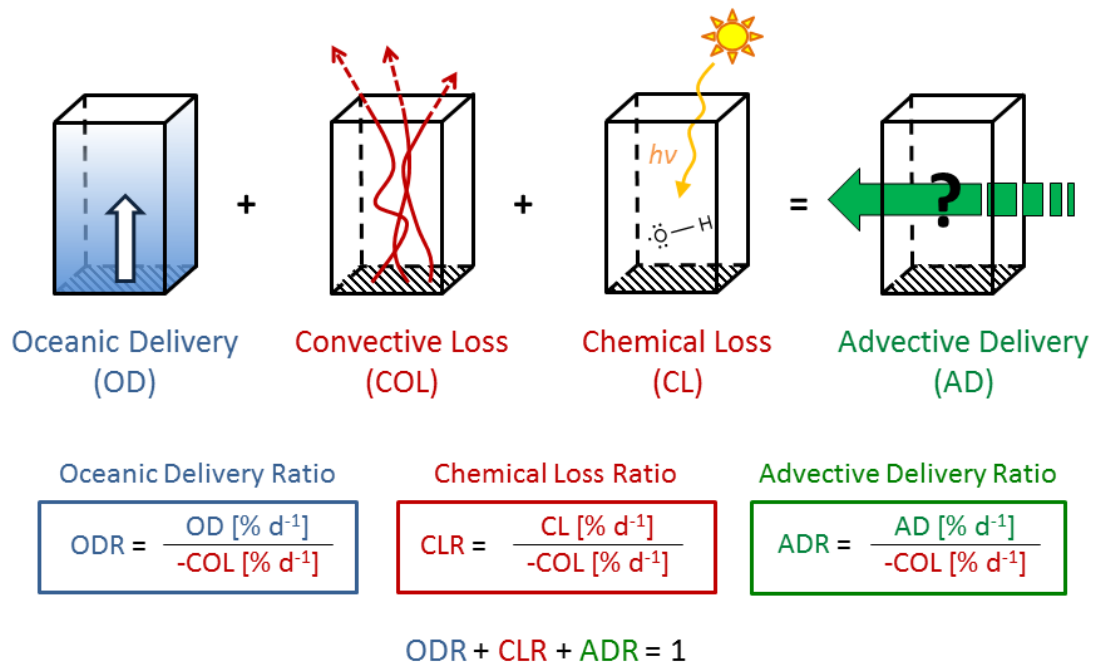


Figure 1: Schematic summary of the components of the applied mass-balance concept: Oceanic Delivery (OD), the Convective Loss (COL), the Chemical Loss (CL), the Advective Delivery (AD), the Oceanic Delivery Ratio (ODR), the Chemical Loss Ratio (CLR) and the Advective Delivery Ratio (ADR). The shaded area reflects an area of 400 m<sup>2</sup>.

2. P. 20599, line 1, replace “more” with “other”

Done.

3. P. 20600, line 13-14, delete “respectively”

Done.

4. P. 20600, lines 15-19, delete all

Since this part gives an overview of the manuscript structure we would like to keep this part.

5. P. 20600, line 23, replace “ships” with “ship”

Done.

6. P. 20601, line 21, replace “from” with “near”

Done.

7. P. 20603, line 3, how high is the 5th superstructure, what obstacles surround it, etc.?

The 5<sup>th</sup> superstructure deck on R/V METEOR is found at about 20m above sea level. A smaller 6<sup>th</sup> superstructure deck with additional masts is found above it. More information can be found at: <https://www.lfd.uni-hamburg.de/en/meteor/technisches.html>.

A jib was used to sample the VSLs freely about 5 – 6 m portside, to avoid any ship influences on the measurements. We added this to the manuscript.

8. P. 20603, line 11, define “moon pool”

A moon pool (hydrographic shaft) is an opening in the base of the ship hull that gives access to the water below, providing protection for the sampling instruments. We added this information to the manuscript:

“102 water samples were taken 3 hourly at a depth of 6.8 m from a continuously working water pump in the hydrographic shaft, an opening in the base of the ship hull of R/V Meteor, after December 9, 2012.”

9. P. 20604, lines 10,11, remove sentence, place refs at end of previous sentence.

Done.

10. P. 20604 lines 22, 23, move “from the ocean surface to right after “launched”; make “positions” singular.

Done.

11. P. 20606, line 1, replace “relating” with “ratioing”; replace “receive” with “estimate”.

Done.

12. P. 20606, line 3, delete “respectively”

Done.

13. P. 20606, lines 1-5. This part is confusing and a good place where the diagram could be put to use.

We will insert the new diagram at this point.

14. P. 20606, line 23, how much of a temperature drop was it to get to 18 degrees?

This depends on the region. Generally outside the upwelling area, the SST ranges between 19 and 22 °C. We added this information to the manuscript:

“The most intense upwelling is observed for several times near the coast where both, SST and SAT rapidly drop from 19 – 22 °C to less than 18 °C (Figure 3a).”

15. P. 20607, lines 1-10, Could this be reduced to a simple sentence?

We think that the relation between absolute and relative humidity and their indication of different air masses might not be trivial for all readers and thus like to keep this part in the manuscript.

16. P. 20607, lines 12-18, *Is this paragraph necessary? Similarly, is the next one necessary? Can the authors simply make a few statements about the meaning of these concentrations, how they relate to other areas, and how they might be useful to support their conclusions? Numbers are best placed in tables so the authors can refer to them and keep the text focused on the issues at hand.*

We agree with the reviewer and shortened the first and second paragraph accordingly. We also cut out repeated numbers and refer to the responding tables.

“Surface bromoform concentrations in the Peruvian upwelling are generally lower during the cruise compared to the Mauritanian upwelling while dibromomethane surface water concentrations are comparable. However, methyl iodide concentrations are almost 8 times higher than in the Mauritanian upwelling (Figure 3d, Table 1, Hepach et al., 2014). Samples taken in the upwelling areas show elevated concentrations compared to the open ocean for all compounds. For further discussion on the distribution of the oceanic halocarbons, see Hepach et al. (2016, submitted to ACPD).

Atmospheric mixing ratios of  $\text{CHBr}_3$  are on average  $2.91 \pm 0.68$  ppt (Table 1).  $\text{CH}_2\text{Br}_2$  mixing ratios of  $1.25 \pm 0.26$  ppt are low and show a similar temporal pattern with bromoform (Table 3). Mixing ratios of both compounds are significantly lower above the Peruvian upwelling compared to observations above the Mauritanian upwelling, while  $\text{CH}_3\text{I}$  mixing ratios are comparable (Fuhlbrügge et al., 2013). Elevated mixing ratios for all three compounds are generally found above intense cold oceanic upwelling regions close to the Peruvian coast (Figure 3e). While the bromocarbons double above the upwelling, methyl iodide mixing ratios increase up to 5-fold, showing its stronger accumulation in the low boundary layer.

The concentration ratio of dibromomethane and bromoform can be used as an indicator of fresh bromocarbon sources along coastal areas. Low ratios of about 0.1 have been observed at coastal source regions and are interpreted as the emission ratios of macro algae (Yokouchi et al., 2005; Carpenter et al., 2003). The applied shorter mean lifetime of bromoform (15 days) in contrast to dibromomethane (94 days) in the boundary layer after Carpenter et al. (2014) leads to an increase of the ratio during transport as long as the air mass is not enriched with fresh bromoform. A general decrease of the concentration ratio is found from the North to the South during the cruise (Figure 3f), implying relatively remote air masses in the North and an intensification of fresh sources towards the South, which is also reflected by elevated water

concentrations towards the South. Atmospheric methyl iodide measurements along the cruise track reveal a mean mixing ratio of  $1.54 \pm 0.49$  ppt, which, similar to the two bromocarbons, maximizes over the coastal upwelling regions (Figure 3e).”

*17. P. 20608, lines 23-25, This is a strange statement in that it is obvious. MBL concentrations are always a function of air-sea differences, in situ loss, and advection. The sentence after this is equally unnecessary.*

We agree and removed the sentences.

*18. P. 20609, all, This tutorial discussion could be condensed to a few sentences, in my mind. If the authors are trying to explain the 15-16 December anomaly, they should focus on that, not ramble through all the rest.*

In this part we describe the overall atmospheric conditions (not only 15-16 December), which significantly influence surface VSLs abundances in this region, and the methodology to explain how the missing MABL heights were calculated. Although we think this part is necessary we shortened the section according to the reviewer’s suggestion and rewrote this section to:

### “3.3 Lower atmospheric conditions

The relative humidity shows a strong vertical gradient from over 75 % to less than 50 % at ~1 km height (Figure 4a) which indicates an increase of the atmospheric stability with height due to suppressed mixing. This convective barrier, known as the trade inversion (Riehl, 1954, 1979; Höflich, 1972), is also reflected in the meridional wind (Figure 4b). Below ~1 km altitude the Southeast trade winds create a strong positive meridional wind component, also visible in the forward trajectories (Figure 2c-d). The flow of air masses in the Hadley Cell back to the subtropics causes a predominantly northerly wind above ~1 km height. The intense increase of  $\theta_v$  in combination with the relative humidity decrease and the wind shear at ~1 km height identifies this level as a strong vertical transport barrier (Figure 4c). Above the cold upwelling water, temperature inversions create additional stable layers above the surface, leading to very low MABL heights of < 100 m, e.g., on December 03, 08 or 17, 2012 and to a reduced vertical transport of surface air. The mean MABL height from the

radiosonde observations is  $370 \pm 170$  m (ERA-Interim  $376 \pm 169$  m). The relative humidity, SAT, SST and wind speed are good indicators for the MABL conditions in this oceanic region and these meteorological parameters show significant correlations with the observed MABL height (Table 3). Thus, we use a multiple linear regression based on these parameters to estimate the MABL height above the coastal upwelling (Section 2.2.2). The regressed MABL heights above the cold upwelling regions are  $158 \pm 79$  m and go down to even 10 m as was previously observed above the Mauritanian Upwelling (Fuhlbrügge et al., 2013). With the regressed MABL heights, the mean MABL height during the cruise decreases to  $307 \pm 177$  m. The stable atmospheric conditions from the surface to the trade inversion lead to strong transport barriers and to a suppressed transport of surface and MABL air into the free troposphere (Figure 4d).”

*19. P. 20610, lines 9-16, This is good and relevant.*

Thank you.

*20. P. 20610, lines 25 ff, This is where the authors need to insert some perspective as discussed under General Comments. Also, how much of the discussion on the following page is relevant to their main point?*

We included the following sentences on page 20611, line 2:

“Generally, the low ODRs along the cruise track are caused by the relatively low oceanic emissions. Since the observed atmospheric concentrations cannot be explained by the local oceanic emissions advection leads to the background concentrations of  $\text{CH}_2\text{Br}_2$  and  $\text{CHBr}_3$ . According to the backward trajectories, potential source regions may be found closer to the coast and to the South. The elevations of the atmospheric mixing ratios above the cold coastal upwelling can partly be explained by accumulation of local oceanic emissions in the stable low MABL. However, as the emissions appear generally not strong enough, except for methyl iodide, to explain the mixing ratios, the contribution of coastal sources is very likely (Figure 2b).”

And on page 20611, line 13:

“These numbers imply that observed VSLS concentrations are advected below the trade inversion in the more open ocean regions during the cruise. An overall discussion is given in Section 4.”

The remaining sentences of section 3.4 are removed (line 13-20).

A more detailed discussion of the phenomena is given within the general comments to the Reviewer 2 above and in the detailed discussion in Section 4 of the manuscript.

*21. P. 20611-12, Section 3.5. Numbers are getting in the way of the points the authors need to make. There is a table of correlation coefficients. The authors should make the important points and simply refer to the table.*

We agree and removed the numbers from the text referring to the Table 3, thus the text in the manuscript reduces to:

“Fuhlbrügge et al. (2013) identified the influence of meteorological conditions, in particular of MABL height variations on VSLS abundances in the tropical Northeast Atlantic above the Mauritanian Upwelling, and suggested a general correlation of MABL conditions and VSLS abundances over oceanic upwelling regions. Indeed, we also find significant high correlations between meteorological parameters and the abundances of bromoform, dibromomethane and methyl iodide (Table 3) along the Peruvian coast. The predominantly moderate winds during the cruise are negatively correlated with the atmospheric VSLS and positively correlated with the MABL height. This shows that VSLS abundances tend to be elevated during periods of lower wind speeds which occur also lead to reduced mixing of surface air and therefore to lower MABL heights, in particular above the coastal upwelling events on December 11, 15-17 and 24, 2012, where local sources could accumulate even more. SAT and SST both are negatively correlated with atmospheric VSLS, since elevated atmospheric VSLS mixing ratios are generally found close to the oceanic upwelling regions with low SATs and SSTs. In these regions the decrease of the SATs leads to an increase of the relative humidity (section 3.1), resulting in a significantly high correlation between the surface relative humidity and the VSLS. Since SAT and SST impact the MABL, which affects the relative humidity, these correlation coefficients are co-correlated with each other. Correlation coefficients between the MABL height and the VSLS are slightly lower (Table 3). A principle component analysis of the parameters in Table 3 furthermore underlined a strong connection between SAT, SST,

MABL height, relative humidity and atmospheric mixing ratios of  $\text{CHBr}_3$  and  $\text{CH}_2\text{Br}_2$  (not shown here).

The results reveal that the MABL properties (height and stability) during M91 influence the VSLs abundances at the marine surface, although not as distinct as above the Mauritanian Upwelling during the DRIVE campaign (Fuhlbrügge et al., 2013). A comparison between the observations from this campaign and DRIVE (Figure 5) shows that the lower variance of observations during M91 may explain the lower correlation. Generally higher emissions and occasional lower and even more stable MABL-heights during DRIVE can explain up to 100% of the atmospheric abundances (Fuhlbrügge et al., 2013; Hepach et al., 2014), while during M91 the observed elevations could only partly be explained by the local oceanic emissions.”

*22. P. 20612-20614, Section 4.0, This is where an overall perspective of upwelling contributions and an understanding of overall uncertainties would really help. The authors make some good points here; I'd just like to see them better substantiated.*

We agree and will therefore - in addition to the above discussed method uncertainties (reviewer comment 2) - include the following discussion on page 20614, line 5:

“The contribution of oceanic emissions to the atmospheric mixing ratios in the MABL of the Peruvian upwelling reveals to be rather low in its more open ocean area under the given meteorological conditions. While the cruise track covered a representative area of the Peruvian upwelling elevated oceanic VSLs emissions that could explain the generally high atmospheric VSLs were only observed for methyl iodide. Bromocarbon emissions would have to be two magnitudes larger to explain the observed VMR in the more open ocean regions and a magnitude larger in the direct coastal upwelling regions with low MABL heights. These observations of the brominated compounds need to include upwind advection of elevated sources from the South, and higher elevated coastal emissions not measured during the cruise, while dynamical fluctuations in emissions scenarios close to the cruise time and place may also have to be considered.”

23. P. 20614-20616, too many numbers here. This should be a summary of the main points the authors are trying to make with their data, where the gaps in our understanding still are, what should be done to remedy those gaps, and why. The summary should be much shorter.

We agree and shortened the summary accordingly by i.e. removing most numbers and concentrating on the main points:

“This study investigated the contribution of oceanic emissions to VSLs abundances in the lowermost atmosphere as well as meteorological constraints on this contribution above both, coastal upwelling and open ocean along the Peruvian coast during December 2012. Meteorological data were obtained on R/V METEOR near the ocean surface and by radiosondes up to the stratosphere. Oceanic VSLs emissions along the cruise track were determined from air and surface water data. The transport of air masses was determined with FLEXPART trajectories.

Oceanic upwelling was observed close to the Peruvian coast. On average a low, stable MABL height of  $307 \pm 177$  m was encountered during the cruise, decreasing to on average 100 m above the upwelling. A distinct trade inversion at  $1.1 \pm 0.3$  km height evolved as the dominant transport barrier for MABL air into the free troposphere during the cruise. The halogenated VSLs bromoform and dibromomethane showed low oceanic emissions of  $117 \pm 492$  pmol m<sup>-2</sup> hr<sup>-1</sup> for bromoform and  $245 \pm 299$  pmol m<sup>-2</sup> hr<sup>-1</sup> for dibromomethane, while methyl iodide emissions were elevated with  $856 \pm 623$  pmol m<sup>-2</sup> hr<sup>-1</sup>. The atmospheric mixing ratios of the compounds were elevated with  $2.9 \pm 0.7$  ppt (bromoform),  $1.3 \pm 0.3$  ppt (dibromomethane) and  $1.5 \pm 0.5$  ppt (methyl iodide). The oceanic emissions along the cruise track explained on average only 3 % (-8 to 33 %) of bromoform, 10 % (-5 to 45 %) of dibromomethane, and 28 % (3 to 80 %) of methyl iodide abundances in the MABL. Thus, the expected significant contribution of local oceanic VSLs emissions from the Peruvian upwelling to the overlying atmosphere was not captured during the time and location of the cruise. The elevated atmospheric VSLs mixing ratios above the Peruvian upwelling therefore appear largely advected and enriched along the Peruvian coast before reaching the ship. Additional potential source regions must exist closer to the coast and also further South of the cruise track along the coast line. Nevertheless, significant correlations between the MABL height and marine atmospheric abundances of the VSLs reveal an impact of the oceanic emissions on the atmospheric VSLs mixing ratio variations.

Our study confirms that MABL height and stability are generally related with atmospheric VSLs abundances above oceanic upwelling regions. Additionally, a widespread trade

inversion can lead to a near-surface accumulation of the VSLS and thus also impact oceanic emissions. Despite the observed elevated atmospheric concentrations during the cruise, a significant contribution of oceanic emissions to the atmosphere, in particular of the bromocarbons  $\text{CHBr}_3$  and  $\text{CH}_2\text{Br}_2$ , was not identified in the observed area during the time of the cruise. Further studies are necessary to clearly uncover the source regions of the elevated atmospheric VSLS in the Peruvian upwelling. Also the double transport barrier phenomena should be investigated in future studies of other oceanic upwelling regions as well. “

## References

- Carpenter, L., Liss, P., and Penkett, S.: Marine organohalogens in the atmosphere over the Atlantic and Southern Oceans, *Journal of Geophysical Research-Atmospheres*, 108, 10.1029/2002JD002769, 2003.
- Carpenter, L. J., Reimann, S., Burkholder, J. B., Clerbaux, C., Hall, B. D., Hossaini, R., Laube, J. C., and Yvon-Lewis, S. A.: Update on Ozone-Depleting Substances (ODSs) and Other Gases of Interest to the Montreal Protocol, in: *Scientific Assessment of Ozone Depletion: 2014*, edited by: Engel, A., and Montzka, S. A., World Meteorological Organization, Geneva, 2014.
- Fuhlbrügge, S., Krüger, K., Quack, B., Atlas, E., Hepach, H., and Ziska, F.: Impact of the marine atmospheric boundary layer conditions on VSLS abundances in the eastern tropical and subtropical North Atlantic Ocean, *Atmospheric Chemistry and Physics*, 13, 6345-6357, 10.5194/acp-13-6345-2013, 2013.
- Fuhlbrügge, S., Quack, B., Tegtmeier, S., Atlas, E., Hepach, H., Shi, Q., Raimund, S., and Krüger, K.: The contribution of oceanic very short lived halocarbons to marine and free troposphere air over the tropical West Pacific, *Atmos. Chem. Phys. Discuss.*, 15, 17887-17943, 10.5194/acpd-15-17887-2015, 2015.
- Hepach, H., Quack, B., Ziska, F., Fuhlbrügge, S., Atlas, E., Krüger, K., Peeken, I., and Wallace, D. W. R.: Drivers of diel and regional variations of halocarbon emissions from the tropical North East Atlantic, *Atmos. Chem. Phys.*, 14, 10.5194/acp-14-1255-2014, 2014.
- Hepach, H., Quack, B., Tegtmeier, S., Engel, A., Bracher, A., Fuhlbrügge, S., L., G., Atlas, E., Lampel, J., Frieß, U., and Krüger, K.: Biogenic halocarbons from the Peruvian upwelling region as tropospheric halogen source, to be submitted, 2016.
- Höflich, O.: The meteorological effects of cold upwelling water areas, *Geoforum*, 3, 35-46, 10.1016/0016-7185(72)90084-X, 1972.
- Lennartz, S. T., Krysztofiak, G., Marandino, C. A., Sinnhuber, B. M., Tegtmeier, S., Ziska, F., Hossaini, R., Krüger, K., Montzka, S. A., Atlas, E., Oram, D. E., Keber, T., Bönisch, H., and Quack, B.: Modelling marine emissions and atmospheric distributions of halocarbons and dimethyl sulfide: the influence of prescribed water concentration vs. prescribed emissions, *Atmos. Chem. Phys.*, 15, 11753-11772, 10.5194/acp-15-11753-2015, 2015.
- Liss, P. S., and Merlivat, L.: Air-Sea Gas Exchange Rates: Introduction and Synthesis, in: *The Role of Air-Sea Exchange in Geochemical Cycling*, edited by: Buat-Menard, P., Reidel, D., and Norwell, M., Springer Netherlands, 113-127, 1986.
- Riehl, H.: *Tropical meteorology*, McGraw-Hill, New York-London, 1954.
- Riehl, H.: *Climate and Weather in the Tropics*, Academic Press, London, 1979.
- Wanninkhof, R., and McGillis, W.: A cubic relationship between air-sea  $\text{CO}_2$  exchange and wind speed, *Geophysical Research Letters*, 26, 1889-1892, 10.1029/1999GL900363, 1999.

Yokouchi, Y., Hasebe, F., Fujiwara, M., Takashima, H., Shiotani, M., Nishi, N., Kanaya, Y., Hashimoto, S., Fraser, P., Toom-Sauntry, D., Mukai, H., and Nojiri, Y.: Correlations and emission ratios among bromoform, dibromochloromethane, and dibromomethane in the atmosphere, *Journal of Geophysical Research-Atmospheres*, 110, 10.1029/2005JD006303, 2005.

## Relevant changes made in the manuscript:

- Section 3.2, 3.3, 3.5 and 5 have been revised, shortened and streamlined
- In Section 3.4 an explanation for the ODR results has been added
- An uncertainty discussion regarding our method has been added to Section 4
- Updating our results with most current lifetime estimates of bromoform, dibromomethane and methyl iodide from the WMO, 2014.
- Air-sea fluxes in the manuscript have been recalculated using the wind speed at 10m height instead of 25 m for the wind based transfer coefficient  $k_w$ .
- Figures:
  - Figure 1 is new
  - Figure 2 is now Figure 3
  - Figure 3 is now Figure 4
  - Figure 4 is now Figure 5, in addition we revised the colours and legend.

All changes are marked-up (red: removed, blue: rewritten/new) in the following:

# 1 Meteorological constraints on oceanic halocarbons above the Peruvian 2 Upwelling

3

4 **S. Fuhlbrügge<sup>1</sup>, B. Quack<sup>1</sup>, E. Atlas<sup>2</sup>, A. Fiehn<sup>1</sup>, H. Hepach<sup>1</sup>, K. Krüger<sup>3</sup>**

5 [1] GEOMAR | Helmholtz Centre for Ocean Research Kiel

6 [2] Rosenstiel School for Marine and Atmospheric Sciences, Miami, Florida

7 [3] University of Oslo, Oslo, Norway

8 Correspondence to: K. Krüger (kirstin.krueger@geo.uio.no)

9

## 10 **Abstract**

11 Halogenated very short lived substances (VSLS) are naturally produced in the ocean and  
12 emitted to the atmosphere. Recently, oceanic upwelling regions in the tropical East Atlantic  
13 were identified as strong sources of brominated halocarbons to the atmosphere. During a  
14 cruise of R/V METEOR in December 2012 the oceanic sources and emissions of various  
15 halogenated trace gases and their mixing ratios in the marine atmospheric boundary layer  
16 (MABL) were investigated above the Peruvian Upwelling for the first time. This study  
17 presents novel observations of the three VSLS bromoform, dibromomethane and methyl  
18 iodide together with high resolution meteorological measurements and Lagrangian transport  
19 modelling. Although relatively low oceanic emissions were observed, except for methyl  
20 iodide, surface atmospheric abundances were elevated. Radiosonde launches during the  
21 cruise revealed a low, stable MABL and a distinct trade inversion above acting both as strong  
22 barriers for convection and trace gas transport in this region. Significant correlations between  
23 observed atmospheric VSLS abundances, sea surface temperature, relative humidity and  
24 MABL height were found. We used a simple source-loss estimate to identify the contribution  
25 of oceanic emissions to observed atmospheric concentrations which revealed that the  
26 observed marine VSLS abundances were dominated by horizontal advection below the trade  
27 inversion. The observed VSLS variations can be explained by the low emissions and their  
28 accumulation under different MABL and trade inversion conditions. This study confirms the  
29 importance of oceanic upwelling and trade wind systems on creating effective transport

30 barriers in the lower atmosphere controlling the distribution of VSLs abundances above  
31 ocean upwelling regions.

32

### 33 **1. Introduction**

34 Short-lived halocarbons from the oceans contribute to reactive atmospheric halogens, which  
35 are involved in tropospheric and stratospheric ozone depletion, aerosol formation, and ~~more~~  
36 ~~other~~ chemical cycles, influencing the fate of pollutants and climate (McGivern et al.,  
37 2000; Saiz-Lopez and von Glasow, 2012; Simpson et al., 2015). Recent studies have identified  
38 open ocean upwelling areas in the Atlantic as large source regions for a number of  
39 brominated and iodinated oceanic trace gases (Quack et al., 2004; Quack et al., 2007; O'Brien  
40 et al., 2009; Raimund et al., 2011; Hepach et al., 2015a). Their sources are related to biological  
41 and chemical processes in the productive waters of the upwelling. The compounds are  
42 emitted from the ocean and are horizontally transported and vertically mixed in the marine  
43 atmospheric boundary layer (MABL) (Carpenter et al., 2010). In the Mauritanian upwelling,  
44 it was found that besides oceanic sources meteorological conditions strongly influenced the  
45 atmospheric mixing ratio of the marine compounds bromoform ( $\text{CHBr}_3$ ), dibromomethane  
46 ( $\text{CH}_2\text{Br}_2$ ) and also methyl iodide ( $\text{CH}_3\text{I}$ ) (Hepach et al., 2014). Especially the combination of  
47 a pronounced low MABL above cold upwelling waters with high concentrations and  
48 emissions of the compounds caused elevated atmospheric mixing ratios. In return, these  
49 atmospheric mixing ratios also reduce the marine emissions through a decrease of the sea-air  
50 concentration gradient (Fuhlbrügge et al., 2013). Similar relationships would be expected for  
51 other oceanic upwelling areas, where not only the oceanic emissions, but also meteorological  
52 conditions in the lowermost atmosphere, i.e., the height, type and structure of the boundary  
53 layer and trade inversion, determine the VSLs contribution to atmospheric chemical  
54 processes. The intense oceanic upwelling in the Southeast Pacific off the coast of Peru  
55 transports large amounts of subsurface waters to the ocean surface and creates one of the  
56 highest productive oceanic regions worldwide (Codispoti et al., 1982). The Peruvian  
57 Upwelling is therefore a potentially intense source region for halogenated VSLs, e.g.  
58 bromoform ( ~~$\text{CHBr}_3$~~ ), dibromomethane ( ~~$\text{CH}_2\text{Br}_2$~~ ) and methyl iodide ( ~~$\text{CH}_3\text{I}$~~ ) (Yokouchi et al.,  
59 1999; Butler et al., 2007; Carpenter et al., 2009). Indeed, Schönhardt et al. (2008) detected  
60 elevated IO columns during September and November 2005 along the Peruvian coast with  
61 the SCIAMACHY satellite instrument and implied elevated iodine source gases from the  
62 Peruvian Upwelling.

63 Although, recent studies investigated halocarbons in the East Pacific (Yokouchi et al.,  
64 2008;Mahajan et al., 2012;Saiz-Lopez et al., 2012;Gómez Martin et al., 2013;Liu et al., 2013)  
65 few studies concentrated on the Peruvian Upwelling in the Southeast Pacific. Only  
66 measurements of methyl iodide exist in this region, revealing atmospheric abundances of 7  
67 ppt (Rasmussen et al., 1982). Observations of bromocarbons above the Peruvian Upwelling  
68 are lacking.

69 In this study we present a high resolution dataset of meteorological parameters, oceanic  
70 concentrations, emissions and atmospheric abundances of VSLS along the Peruvian coast and  
71 in the Upwelling. Not much is known of the oceanic source strength of the VSLS and the  
72 meteorological influence on the marine trace gas distribution and abundances in this region.  
73 The goal of this study is to assess the influence of oceanic upwelling and meteorological  
74 conditions on the atmospheric VSLS abundances above the Peruvian Upwelling, and the  
75 contribution of the local oceanic emissions to ~~, respectively the MABL mixing ratios, and to~~  
76 free tropospheric VSLS concentrations.

77 The paper is structured as following. Chapter 2 gives an overview of the data and methods we  
78 use in this study. Chapter 3 presents the results from our atmospheric and oceanic  
79 observations and analyses the contribution from oceanic VSLS emissions to the MABL, as  
80 well as meteorological constrains on the observations. Chapter 4 discusses the results, before  
81 the study is summarized in Chapter 5.

82

## 83 **2. Data and Methods**

84 The cruise M91 on R/V METEOR from December 01 to 26, 2012 started and ended in Lima,  
85 Peru ~~(Figure 1a)~~. The ship reached the most northern position during the cruise on December  
86 03, 2012 at 5° S. In the following three weeks the ships headed southward and reached its  
87 southern most position at 16° S on December 21, 2012. During this time the track alternated  
88 between open ocean sections and sections very close to the Peruvian coast in the cold  
89 upwelling waters to collect coastal as well as open ocean data. Diurnal variations were  
90 observed during 6 stations along the cruise track ~~(Figure 2)~~.

91

### 92 **2.1 Meteorological observations**

93 Meteorological measurements of surface air temperature (SAT), sea surface temperature  
94 (SST), relative humidity, air pressure, wind speed and direction were taken every second at  
95 about 25 m height on R/V METEOR and averaged to 10 minute intervals for our  
96 investigations. Atmospheric profiles of temperature, wind and humidity were obtained by 98

97 radiosonde launches at standard UTC time (0, 6, 12, 18 UTC) and additionally 3 hourly  
98 during the diurnal stations along the cruise track, using Vaisala RS92 radiosondes. Due to  
99 permission limitations, radiosondes could not be launched within 12 nautical miles of the  
100 Peruvian coast. The collected radiosonde data was integrated in near real time into the Global  
101 Telecommunication System (GTS) to improve meteorological reanalysis (e.g. ERA-Interim)  
102 and operational European Centre for Medium Range Weather Forecast models (opECMWF).

103

## 104 **2.2 MABL height**

105 The radiosonde data are used to identify the height of the MABL, which is the atmospheric  
106 surface layer above the ocean in which trace gas emissions are mixed horizontally on a short  
107 time scale of an hour or less by convection and turbulence (Stull, 1988). Two different kinds  
108 of MABL can be distinguished, the convective and the stable MABL, which can be  
109 characterized by the gradient of the virtual potential temperature  $\theta_v$ . A negative or neutral  
110 gradient reveals an unstable convective layer, while a positive gradient reveals a stable  
111 atmospheric layer. In case of an increase of the virtual potential temperature ~~from~~ near the  
112 surface, mixing in the MABL is suppressed. The upper limit of the convective MABL is set  
113 by a *stable layer*, e.g., a temperature inversion or a significant reduction in air moisture and is  
114 typically found above open ocean regions between 100 m and 3 km height (Stull,  
115 1988;Seibert et al., 2000). For the determination of this *stable layer* above the convective  
116 MABL, we use the practical approach described in Seibert et al. (2000) and compute the  
117 virtual potential temperature during the radiosonde ascent whose increase with altitude  
118 indicates the base of a *stable layer*. In this study the base of this *stable layer* increased by half  
119 of this *stable layer* depth is the definition for the MABL height. Over oceanic upwelling  
120 regions this stable layer can even descend to the ocean surface (e.g. Höflich et al., 1972 and  
121 Fuhlbrügge et al., 2013).

122

### 123 **2.2.1 Relative humidity**

124 Estimates for atmospheric surface stability and MABL conditions in oceanic upwelling  
125 region can also be obtained from variations of the surface humidity. While the absolute  
126 humidity determines the amount of water in a specific volume of air, the relative humidity is  
127 the ratio of the partial pressure of water vapour to the equilibrium vapour pressure at the  
128 observed temperature. Variations of the SAT therefore directly influence the relative  
129 humidity at the surface. A decrease of the SAT due to cold upwelling water leads to an  
130 increase of the relative humidity, while the absolute humidity stays constant or even

131 decreases due to condensation of water vapour once the relative humidity reaches 100 % and  
132 the air is saturated with water vapour. An elevated relative humidity in this oceanic region  
133 therefore points to stable layers with suppressed mixing of surface air and to a low and stable  
134 MABL height.

135

### 136 **2.2.2 Estimation of MABL height above the upwelling**

137 To estimate the MABL height above upwelling areas close to the coast, where radiosonde  
138 launches were permitted (Section 2.1) a multiple linear regression was applied. Using  
139 observed meteorological parameters revealing significant correlations (see Section 3.5) with  
140 the observed MABL height, relative humidity ( $x_1$ ), SAT ( $x_2$ ), SST ( $x_3$ ) and wind speed ( $x_4$ ),  
141 along the cruise we obtained the following Eq. 1:

142

$$MABL\ height = b_1x_1 + b_2x_2 + b_3x_3 + b_4x_4 \quad (Eq. 1)$$

with  $b_1 = -0.0117$ ;  $b_2 = 0.0202$ ;  $b_3 = 0.0467$ ;  $b_4 = 0.0089$

143

### 144 **2.3 Atmospheric VLS measurements**

145 A total of 198 air samples were collected 3 hourly during the cruise at about 20 m height on  
146 the 5<sup>th</sup> superstructure deck of R/V METEOR using a portside jib of 5 – 6 m. The air samples  
147 were pressurized to 2 atm in pre-cleaned stainless steel canisters with a metal bellows pump  
148 and were ~~analyzed~~ analysed at the Rosenstiel School for Marine and Atmospheric Sciences  
149 (RSMAS, Miami, Florida) within 6 months after the cruise. Details about the analysis, the  
150 instrumental precision and the preparation of the samples are described in Schaufliet et al.  
151 (1999) and Fuhlbrügge et al. (2013). The atmospheric mixing ratios were calculated with a  
152 NOAA standard (SX3573) from GEOMAR.

153

### 154 **2.4 Oceanic concentrations and sea – air flux**

155 102 water samples were taken ~~in-situ on a~~ 3 hourly at a depth of 6.8 m from a continuously  
156 working water pump in the hydrographic shaft, ~~basis from the moon pool~~ an opening in the  
157 base of the ship hull of R/V Meteor, ~~at a depth of 6.8 m from a continuously working water~~  
158 ~~pump~~ after December 9, 2012. The samples were then analysed for bromoform,  
159 dibromomethane and methyl iodide and other halogenated trace gases by a purge and trap  
160 system, attached to a gas chromatograph combined with an ECD (electron capture detector)

161 with a precision of 10 % determined from duplicates. The approach is described in detail by  
162 Hepach et al. (2014).

163

#### 164 **2.4.1 Sea – air flux**

165 The sea – air flux ( $F$ ) of bromoform, dibromomethane and methyl iodide is calculated with  $k_w$   
166 as transfer coefficient and  $\Delta c$  as concentration gradient between the water and equilibrium  
167 water concentration determined from the atmospheric concentrations (Eq. 2). The transfer  
168 coefficient was determined by the air – sea gas exchange parameterization of Nightingale et  
169 al. (2000) after a Schmidt number ( $Sc$ ) correction for the three gases (Eq. 3).

170

$$F = k_w \cdot \Delta c \quad (\text{Eq. 2})$$

171

$$k_w = k_{CO_2} \cdot \frac{Sc^{-\frac{1}{2}}}{600} \quad (\text{Eq. 3})$$

172

173 Details on deriving the air – sea concentration gradient and emissions are further described in  
174 Hepach et al. (2014) and references therein.

175

#### 176 **2.5 Trajectory calculations**

177 The Lagrangian Particle Dispersion Model FLEXPART of the Norwegian Institute for Air  
178 Research in the Department of Atmospheric and Climate Research (Stohl et al., 2005) was  
179 used to analyse the air mass origins and the transport of surface air masses along the cruise  
180 track to the free troposphere ~~-FLEXPART has been evaluated in previous studies-~~ (Stohl et  
181 al., 1998;Stohl and Trickl, 1999). The model includes moist convection and turbulence  
182 parameterizations in the atmospheric boundary layer and free troposphere (Stohl and  
183 Thomson, 1999;Forster et al., 2007). We use the ECMWF (European Centre for Medium-  
184 Range Weather Forecasts) reanalysis product ERA-Interim (Dee et al., 2011) with a  
185 horizontal resolution of  $1^\circ \times 1^\circ$  and 60 vertical model levels as meteorological input fields,  
186 providing air temperature, horizontal and vertical winds, boundary layer height, specific  
187 humidity, as well as convective and large scale precipitation with a 6 hourly temporal  
188 resolution. Due to the spatial resolution of ERA-Interim data along the Peruvian coast  
189 defining the land-sea mask of our trajectory calculations, 98 out of 140 release points for the  
190 forward and backward trajectory calculations were analysed along the cruise track. At each  
191 these release points 10,000 forward and 50 backward trajectories were launched from the

192 | ocean surface within  $\pm 30$  minutes and  $\sim 20$  m distance to the ship positions ~~from the ocean~~  
193 | ~~surface~~. Time and position of the release events are synchronized with air samples taken on  
194 | R/V METEOR (Section 2.3~~2.3~~).

195

## 196 | **2.6 Oceanic contribution to MABL VSLS abundances**

197 | To obtain an estimate of the contribution of local oceanic sources to the atmospheric mixing  
198 | ratios in the lowermost atmosphere above the Peruvian upwelling we apply a mass balance  
199 | concept to the oceanic emissions, to the time scales of air mass transport and to the chemical  
200 | loss (Fuhlbrügge et al., 2015). First we define a box above each release event with a size of  
201 |  $\sim 400 \text{ m}^2$  around the measurement location and the height of the MABL and assume a steady-  
202 | state observed VSLS mixing ratio within the box (Figure 1). During each trajectory release  
203 | event we assume the specific sea-air flux to be constant and the emissions to be  
204 | homogeneously mixed within the box. Then the contribution of the sea-air flux is computed  
205 | as the ratio of the VSLS flux from the ocean into the MABL (in mol per day) and the total  
206 | amount of VSLS in the box (in mol) and is defined as the Oceanic Delivery (OD) and OD is  
207 | given in percentage per day. In addition to the delivery of oceanic VSLS to the box, the loss  
208 | of VSLS out of the box into the free troposphere is defined as the CONvective Loss (COL)  
209 | and is derived from the mean residence time derived from the FLEXPART trajectories in the  
210 | box during each release event. Since this process is a loss process, COL is given as a negative  
211 | quantity and in percentage per day. The chemical degradation of VSLS by OH and photolysis  
212 | in the MABL is considered by the chemical lifetime of each compound in the MABL. We use  
213 | lifetimes of 16 days for bromoform and 60 days for dibromomethane (Hossaini et al., 2010)  
214 | and 3 days for methyl iodide (R. Hossaini, personal communication), representative for the  
215 | tropical boundary layer. The Chemical Loss (CL) acts as loss process as well and is given as  
216 | a negative quantity in percentage per day. We further assume a steady state in the box. OD,  
217 | COL and CL must therefore be balanced by an advective transport of air masses in and out of  
218 | the box. The change of the VSLS through advective transport is defined as Advective  
219 | Delivery (AD) and given in percentage per day.

220 | By ~~relating ratioing~~ OD to COL, we ~~receive estimate~~ an Oceanic Delivery Ratio (ODR) (Eq.  
221 | 4):

222

$$ODR = \frac{OD [\%d^{-1}]}{-COL [\%d^{-1}]} = \frac{Sea-Air \text{ flux contribution } [\%d^{-1}]}{Loss \text{ of box air to the FT } [\%d^{-1}]} \quad (\text{Eq. 4})$$

223

224 | Similarly, the Chemical Loss in the box (CL) and ~~respectively~~, the change in VSLs due to  
225 | advection (AD) are related to COL to get the Chemical Loss Ratio (CLR) and the Advective  
226 | Delivery Ratio (ADR) with  $ADR = 1 - CLR - ODR$ . Since CL, OD and AD are divided by –  
227 | COL, ratios for source processes are positive and negative for loss processes (Fuhlbrügge et  
228 | al., 2015).

229

### 230 | 3. Observations on R/V METEOR

#### 231 | 3.1. Meteorological observations

232 | The Peruvian coast is dominated by the southern hemisphere trade wind regime with  
233 | predominantly southeast winds (Figure 2~~Figure 1~~). The Andes, which are known to act as a  
234 | barrier to zonal wind in this region, affect the horizontal air mass transport along the coast  
235 | (Figure 2~~Figure 1~~b-d). The steeply sloping mountains at the coast form strong winds parallel  
236 | to the South American coastline (Garreaud and Munoz, 2005), leading to distinct wind-driven  
237 | oceanic upwelling of cold water along the coast. The 10-day backward trajectories reveal  
238 | predominantly near-shore air masses with coastal influence and marine air masses (Figure  
239 | 2~~Figure 1~~). The average wind direction observed on R/V Meteor during the cruise is  $160^\circ \pm$   
240 |  $34^\circ$  (mean  $\pm \sigma$ ) with a moderate average wind speed of  $6.2 \pm 2.2 \text{ ms}^{-1}$  (Figure 3~~Figure 2~~b).  
241 | ERA-Interim reveals similar winds along the cruise track with a mean wind speed of  $5.6 \pm$   
242 |  $1.8 \text{ ms}^{-1}$  and a mean wind direction of  $168^\circ \pm 21^\circ$  (not shown here). The divergence of the  
243 | wind driven Ekman transport along the Peruvian coast leads to the observed oceanic  
244 | upwelling of cold waters. The most intense upwelling is observed for several times near the  
245 | coast where both, SST and SAT rapidly drop from  $19 - 22^\circ \text{C}$  to less than  $18^\circ \text{C}$  (Figure  
246 | 3a).~~This upwelling is observed for several times near the coast where both, SST and SAT~~  
247 | ~~rapidly drop to less than  $18^\circ \text{C}$  (Figure 2a).~~ The impact of the cold upwelling water on the  
248 | observed air masses is also visible in the observed humidity fields (Figure 3~~Figure 2~~c). Here,  
249 | the decreasing SAT reduces the amount of water vapour that the surface air is able to contain,  
250 | leading to an increase of the relative humidity. The decreasing SAT and increasing relative  
251 | humidity above the oceanic upwelling indicate a stable atmospheric surface layer with ~~in~~  
252 | ~~which~~suppressed vertical mixing ~~is suppressed~~. The absolute humidity stays constant or even  
253 | decreases above the oceanic upwelling due to condensation of water vapour when surface air  
254 | cools and becomes saturated, which coincides with fog observations on the ship above the  
255 | upwelling regions. A decrease of the absolute humidity outside the upwelling points to a  
256 | change in advected air masses for example between December 9 and 11, but also on  
257 | December 19, 2012 (Figure 3~~Figure 2~~c).

258

### 259 3.2. VLSL observations and oceanic emissions

260 Surface bromoform concentrations in the Peruvian upwelling ~~ocean surface~~ are generally  
261 lower during the cruise compared to the Mauritanian upwelling while dibromomethane  
262 surface water concentrations are comparable ~~range from 0.2–21.5 pmol L<sup>-1</sup> with a mean of~~  
263 ~~6.6 ± 5.5 (1σ) pmol L<sup>-1</sup> during the cruise (Figure 2d, Table 1).~~ However methyl iodide  
264 concentrations are almost 8 times higher than in the Mauritanian upwelling (Figure 3d, Table  
265 1, Hepach et al., 2014). ~~Dibromomethane concentrations range from 0.2–12.7 pmol L<sup>-1</sup> with~~  
266 ~~a mean of 4.3 ± 3.4 pmol L<sup>-1</sup> and methyl iodide concentrations range from 1.1–35.4 pmol L<sup>-1</sup>~~  
267 ~~with a mean of 9.8 ± 6.3 pmol L<sup>-1</sup>.~~ Samples taken in the upwelling areas show elevated  
268 concentrations compared to the open ocean for all compounds. For further discussion on the  
269 distribution of the oceanic halocarbons, see Hepach et al. (2016, submitted to ACPD).

270 ~~Mixing~~ Atmospheric mixing ratios of ~~atmospheric bromoform~~ ~~range from 1.53–5.85 ppt~~  
271 ~~during the cruise with an overall moderate mean of~~ are on average  $2.91 \pm 0.68$  ppt (Table 1).  
272 ~~Elevated mixing ratios of >3 ppt are generally found above the oceanic upwelling areas close~~  
273 ~~to the Peruvian coast, while these concentrations are hardly measured outside the oceanic~~  
274 ~~upwelling (Figure 2e). Highest bromoform mixing ratios (> 4 ppt) are observed on December~~  
275 ~~23 and 24, 2012 at 15.3° S and 75.4° W. Dibromomethane mixing ratios range between 0.82~~  
276 ~~ppt and 2.04 ppt with an mixing ratios of overall low mean of~~  $1.25 \pm 0.26$  ppt ppt are low and  
277 show a similar temporal pattern with bromoform (~~The atmospheric bromocarbons correlate~~  
278 ~~with each other with R = 0.79 (Table 3Table 3).~~ Like bromoform, also dibromomethane  
279 ~~mixing ratios are elevated above the oceanic upwelling areas, except for December 8, 2012,~~  
280 ~~where an increase is also found outside the upwelling.~~ Mixing ratios of both compounds are  
281 significantly lower above the Peruvian upwelling compared to observations above the  
282 Mauritanian upwelling, while methyl iodide mixing ratios are comparable (Fuhlbrügge et al.,  
283 2013). Elevated mixing ratios for all three compounds are generally found above intense cold  
284 oceanic upwelling regions close to the Peruvian coast (Figure 3e). While the bromocarbons  
285 double above the upwelling, methyl iodide mixing ratios increase up to 5-fold, showing its  
286 stronger accumulation in the low boundary layer.

287 The concentration ratio of dibromomethane and bromoform can be used as an indicator of  
288 fresh bromocarbon sources along coastal areas ~~for the age of bromocarbon sources along the~~  
289 ~~coast~~. Low ratios of about 0.1 have been observed at coastal source regions and are  
290 interpreted as the emission ratios of macro algae (Yokouchi et al., 2005; Carpenter et al.,  
291 2003). The applied shorter mean ~~boundary layer~~ lifetime of bromoform (~~16–15~~ days) in

contrast to dibromomethane (60–94 days) in the boundary layer after Hossaini et al. (2010) Carpenter et al. (2014) leads to an increase of the ratio during transport as long as the air mass is not enriched with fresh bromoform. A general decrease of the concentration ratio is found from the North to the South during the cruise (Figure 3f), implying relatively remote air masses in the North and an intensification of fresh sources towards the south, which is also reflected by the elevated water concentrations. ~~During the cruise the concentration ratio shows a gradient from the North to the South, with a mean of  $0.44 \pm 0.07$  (Figure 2f). Thus, we find relatively remote air masses in the North with a concentration ratio of 0.70 on December 5 and lowest ratios down to 0.31 on December 24, 2012, which implies an intensification of fresh sources towards the South that is also reflected by elevated water concentrations.~~ Atmospheric methyl iodide measurements along the cruise track ranges between 0.61 ppt and 3.21 ppt with an overall elevated reveal a mean mixing ratio of  $1.54 \pm 0.49$  ppt, which, similar to the two bromocarbons, ~~generally~~ maximizing over the ~~oceanic~~ upwelling regions (Figure 3 ~~Figure 2e~~). ~~Correlations of methyl iodide with the bromocarbons result in  $R = 0.79$  for bromoform and  $R = 0.66$  for dibromomethane (Table 3).~~ Oceanic emissions during the cruise were calculated from the synchronized measurements of sea water concentrations and atmospheric mixing ratios, sea surface temperatures and wind speeds, measured on R/V METEOR (Section 2.4.1). Oceanic concentrations and atmospheric mixing ratios of each compound are weakly or not at all correlated ( $R_{\text{bromoform}} = 0.00$ ,  $R_{\text{dibromomethane}} = 0.29$  and  $R_{\text{methyl iodide}} = 0.34$ ). Mean sea-air fluxes of the bromocarbons during the cruise are very low with  ~~$130-117 \pm 554-492$  pmol m<sup>-2</sup> hr<sup>-1</sup> (for bromoform), and  $273-245 \pm 334-299$  pmol m<sup>-2</sup> hr<sup>-1</sup> (for dibromomethane),~~ and but for methyl iodide the fluxes are elevated with  $856 \pm 623$  pmol m<sup>-2</sup> h<sup>-1</sup>  ~~$954 \pm 697$  pmol m<sup>-2</sup> hr<sup>-1</sup> (methyl iodide)~~ (Figure 3 ~~Figure 2g~~, Table 1). ~~The low bromocarbon emissions are probably caused by the observed elevated VSLs atmospheric concentrations, relatively low oceanic VSLs concentrations and low wind speeds and SSTs. On the other site, the high concentrations of methyl iodide in the surface waters lead to high oceanic emissions and elevated atmospheric mixing ratios.~~ Further investigations of the distributions and sources of iodinated compounds during this cruise are carried out by Hepach et al. (2015b).

321

### 3.3. Lower atmosphere conditions

The relative humidity shows a strong vertical gradient from over 75 % to less than 50 % at ~1 km height (Figure 4a) which indicates an increase of the atmospheric stability with height due to suppressed mixing. This convective barrier, known as the trade inversion (Riehl, 1954,

1979;Höflich, 1972), is also reflected in the meridional wind (Figure 4b). Below ~1 km altitude the Southeast trade winds create a strong positive meridional wind component, also visible in the forward trajectories (Figure 2c-d). The flow of air masses in the Hadley Cell back to the subtropics causes a predominantly northerly wind above ~1 km height. The intense increase of  $\theta_v$  in combination with the relative humidity decrease and the wind shear at ~1 km height identifies this level as a strong vertical transport barrier (Figure 4c). Above the cold upwelling water, temperature inversions create additional stable layers above the surface, leading to very low MABL heights of < 100 m, e.g., on December 03, 08 or 17, 2012 and to a reduced vertical transport of surface air. The mean MABL height from the radiosonde observations is  $370 \pm 170$  m (ERA-Interim  $376 \pm 169$  m). The relative humidity, SAT, SST and wind speed are good indicators for the MABL conditions in this oceanic region and these meteorological parameters show significant correlations with the observed MABL height (Table 3). Thus, we use a multiple linear regression based on these parameters to estimate the MABL height above the coastal upwelling (Section 2.2.2). The regressed MABL heights above the cold upwelling regions are  $158 \pm 79$  m and go down to even 10 m as was previously observed above the Mauritanian Upwelling (Fuhlbrügge et al., 2013). With the regressed MABL heights, the mean MABL height during the cruise decreases to  $307 \pm 177$  m. The stable atmospheric conditions from the surface to the trade inversion lead to strong transport barriers and to a suppressed transport of surface and MABL air into the free troposphere (Figure 4d).~~The atmospheric conditions in the lower troposphere, in particular the stability of the lowermost atmosphere and the height of the MABL, are obtained from radiosonde data launched along the cruise track. The relative humidity shows a strong vertical gradient at ~1 km height (Figure 3a). At this altitude, the relative humidity drops rapidly from over 75 % to less than 50 % which indicates a decrease in total humidity and/or an increase in air temperature due to suppressed mixing. The barrier for convective activity in this height, known as the trade inversion (Riehl, 1954, 1979;Höflich, 1972), is typically found over the eastern side of tropical oceans within the lower 3 km above the surface and caused by the large scale descending of air masses in the Hadley Cell (Riehl, 1954, 1979). This trade inversion is also reflected in the meridional wind observed by the radiosondes (Figure 3b). Air masses below ~1 km altitude have a strong positive meridional wind component due to the Southeast trade winds in this region, which is also visible in the forward trajectories (Figure 1c-d). The back flow of the trade winds in the Hadley Cell to the subtropics causes a predominantly Northerly wind above ~1 km height. The intense increase of  $\theta_v$  in combination with the relative humidity decrease and the wind shear at ~1 km height identifies this level as~~

~~a strong vertical transport barrier (Figure 3c). However, the low SAT above the cold upwelling water creates additional stable layers below the trade inversion. In particular above the upwelling, these stable layers can reach the surface and lead to very low MABL heights, e.g., on December 03, 08 or 17, 2012 and a reduction in vertical surface air exchange. Meteorological observers on board the ship witnessed fog coinciding with the elevated relative humidity above upwelling regions lasting for almost 20 hours on December 15–16, 2012, confirming the suppressed mixing within the MABL. The mean MABL height from the radiosonde observations is  $370 \pm 170$  m (ERA Interim  $376 \pm 169$  m). Since the relative humidity, SAT, SST and wind speed are good indicators for the MABL conditions in this oceanic region and these meteorological parameters show significant correlations with the observed MABL height (Table 3), we use a multiple linear regression based on these parameters to estimate the MABL height above the upwelling (Section 2.2.2). With the regressed MABL heights above the upwelling, the mean MABL height during the cruise decreases to  $307 \pm 177$  m and reveals the expected low mean MABL heights above cold upwelling regions of  $158 \pm 79$  m and down to even 10 m as was previously observed above the Mauritanian Upwelling (Fuhlbrügge et al., 2013). A 12 hourly ERA-Interim MABL height revealed an average height of  $376 \pm 169$  m along the cruise track. The effects of the MABL and trade inversions transport barriers result in suppressed transport to the free troposphere (Figure 3d).~~

We interpret the observations as the following. In the region of the Peruvian Upwelling, compounds emitted from the ocean and observed at the marine surface are first homogeneously distributed within the MABL during a couple of hours, before advection transport them further within the second transport barrier of the lowermost atmosphere the trade wind inversion. For air masses above or close to oceanic upwelling regions, the MABL height is the first weak transport barrier on short time scales (hours), while the trade inversions acts as the second more pronounced barrier for vertical transport on long time scales (days).

### **3.4. Contribution of oceanic emissions to observed VSLS abundances in the MABL**

We estimate the contribution of oceanic emissions to mixing ratios within the MABL and below the trade inversion with a VSLS source-loss estimate (Table 2). The loss of VSLS out of the MABL box is ~~-34~~<sup>351.7</sup>~~0~~ % d<sup>-1</sup> and equal for all compounds, since it is computed

393 from the loss of trajectories out of the box. The loss is based on a mean residence time of the  
394 FLEXPART trajectories of 7 hours in the observed MABL height during the cruise. The ratio  
395 of the OD of each compound and the COL results in the particular ODR. The ODR reveals  
396 that on average only 3 % of the observed atmospheric bromoform in the MABL origins from  
397 nearby oceanic emissions and that 97–99 % are advected. Local oceanic emissions of  
398 dibromomethane contribute about 44–10 % of the observed abundances in the MABL, while  
399 methyl iodide emissions contribute with 34–28 %, which is far less compared to observations  
400 in other source regions with high convection as in the South China and Sulu Seas  
401 (Fuhlbrügge et al., 2015). Generally, the low ODRs along the cruise track are caused by the  
402 relatively low oceanic emissions. Since the observed atmospheric concentrations cannot be  
403 explained by the local oceanic emissions advection leads to the background concentrations of  
404 bromoform and methyl iodide. According to the backward trajectories, potential source  
405 regions may be found closer to the coast and to the South. The elevations of the atmospheric  
406 mixing ratios above the cold coastal upwelling can partly be explained by accumulation of  
407 local oceanic emissions in the stable low MABL. However, as the emissions appear generally  
408 not strong enough, except for methyl iodide, to explain the mixing ratios, the contribution of  
409 coastal sources is very likely (Figure 2b). While the surface air masses can leave the MABL  
410 within hours, they are suppressed from entering the free troposphere through the trade  
411 inversion barrier. Adapting an average trade inversion height of 1.1 km as the transport  
412 barrier for surface air masses into the free troposphere reveals an average residence time of  
413 the FLEXPART trajectories of 44–48 hrs below this trade inversion height. The atmospheric  
414 VSLs below the trade inversion originate to 42–11 % from oceanic emissions (ODR) for  
415 bromoform, to 37–33 % for dibromomethane and to 103–92 % for methyl iodide. The  
416 increased residence time of air masses below the trade inversion, reflected by the  
417 FLEXPART trajectories, leads to a stronger enrichment of air masses with VSLs from the  
418 oceanic emissions, reflected by OD, compared to the MABL box. However, the low sea-air  
419 fluxes of bromoform and dibromomethane are by far not strong enough to lead to the  
420 observed mixing ratios. These numbers imply that observed VSLs concentrations are  
421 advected below the trade inversion in the more open ocean regions during the cruise. An  
422 overall discussion is given in Section 4. ~~Oceanic emissions of methyl iodide could explain the  
423 atmospheric mixing ratios below the trade inversion (ODR), but the chemical degradation can  
424 destroy up to 72 % (CLR) of the observed amount within the residence time of the air masses  
425 below the trade inversion. Since the oceanic delivery is very low for the bromocarbons and  
426 the elevated oceanic delivery of methyl iodide is nearly compensated by the chemical~~

427 ~~degradation, observed VSLS abundances of all three compounds are mostly advected during~~  
428 ~~the cruise, which is reflected by high ADRs within the MABL and below the trade inversion~~  
429 ~~(Table 2).~~

### 431 **3.5. Meteorological constrains on atmospheric VSLS in the MABL**

432 Fuhlbrügge et al. (2013) identified the influence of meteorological conditions, in particular of  
433 MABL height variations on VSLS abundances in the tropical Northeast Atlantic above the  
434 Mauritanian Upwelling, and suggested a general correlation of MABL conditions and VSLS  
435 abundances over oceanic upwelling regions. Indeed, we also find significant high correlations  
436 between meteorological parameters and the abundances of bromoform, dibromomethane and  
437 methyl iodide (Table 3) along the Peruvian coast. The predominantly moderate winds during  
438 the cruise are negatively correlated with the atmospheric VSLS and positively correlated with  
439 the MABL height. This shows that VSLS abundances tend to be elevated during periods of  
440 lower wind speeds which occur also lead to reduced mixing of surface air and therefore to  
441 lower MABL heights, in particular above the coastal upwelling events on December 11, 15-  
442 17 and 24, 2012, where local sources could accumulate even more. SAT and SST both are  
443 negatively correlated with atmospheric VSLS, since elevated atmospheric VSLS mixing  
444 ratios are generally found close to the oceanic upwelling regions with low SATs and SSTs. In  
445 these regions the decrease of the SATs leads to an increase of the relative humidity (section  
446 3.1), resulting in a significantly high correlation between the surface relative humidity and  
447 the VSLS. Since SAT and SST impact the MABL, which affects the relative humidity, these  
448 correlation coefficients are co-correlated with each other. Correlation coefficients between  
449 the MABL height and the VSLS are slightly lower (Table 3). A principle component analysis  
450 of the parameters in Table 3 furthermore underlined a strong connection between SAT, SST,  
451 MABL height, relative humidity and atmospheric mixing ratios of bromoform and  
452 dibromomethane (not shown here).

453 The results reveal that the MABL properties (height and stability) during M91 influence the  
454 VSLS abundances at the marine surface, although not as distinct as above the Mauritanian  
455 Upwelling during the DRIVE campaign (Fuhlbrügge et al., 2013). A comparison between the  
456 observations from this campaign and DRIVE (Figure 5) shows that the lower variance of  
457 observations during M91 may explain the lower correlation. Generally higher emissions and  
458 occasional lower and even more stable MABL-heights during DRIVE can explain up to  
459 100% of the atmospheric abundances (Fuhlbrügge et al., 2013; Hepach et al., 2014), while

during M91 the observed elevations could only partly be explained by the local oceanic emissions. *et al.* (2013) identified the influence of meteorological conditions, in particular of MABL height variations on VSLS abundances in the tropical Northeast Atlantic above the Mauritanian Upwelling, and suggested a general correlation of MABL conditions and VSLS abundances over oceanic upwelling regions. Indeed, we also find significant high correlations between meteorological parameters and the abundances of bromoform, dibromomethane and methyl iodide (Table 3) along the Peruvian coast. The predominantly moderate winds during the cruise are negatively correlated with the atmospheric VSLS (bromoform  $R = -0.38$ , dibromomethane  $R = -0.53$ , and methyl iodide  $R = -0.33$ ) and positively correlated with the MABL height ( $R = 0.44$ ) implying that VSLS abundances tend to be elevated during periods of lower wind speeds, which in return lead to less mixing of surface air and therefore to lower MABL heights, in particular on December 11, 15-17 and 24, 2012. SAT and SST both correlate with atmospheric VSLS. Bromoform correlates with SAT and SST with  $R = -0.50$ , respectively  $R = -0.57$ . Correlation coefficients between methyl iodide, SAT and SST are slightly lower with  $R = -0.37$  and  $R = -0.42$ , while dibromomethane has the strongest negative correlation to SAT ( $R = -0.78$ ) and SST ( $R = -0.81$ ). Generally high correlations between a meteorological parameter and the VSLS are found for the relative humidity with  $R = 0.74$ ,  $R = 0.77$  and  $R = 0.67$  (bromoform, dibromomethane and methyl iodide). Correlation coefficients between the MABL height and the VSLS are slightly lower with  $R = -0.55$ ,  $R = -0.61$ , respectively  $R = -0.45$ . Since SAT and SST impact the MABL, which affects the relative humidity, these correlation coefficients are co-correlated with each other. The results reveal that the MABL properties (height and character) influence the VSLS abundances at the marine surface, although not as distinct as above the Mauritanian Upwelling (Fuhlbrügge *et al.*, 2013). A comparison between the observations from the Peruvian Upwelling and the Mauritanian Upwelling (Figure 4) shows that the variance of the former may explain the lower correlation. Reasons for this are discussed in the following.

#### 4. Discussion

The observations reveal a significant correlation between the MABL height and atmospheric VSLS abundances above the Peruvian Upwelling. However, the correlation coefficients between the determined MABL height and the atmospheric VSLS are not as high as above the Mauritanian Upwelling during the DRIVE campaign (Fuhlbrügge *et al.*, 2013). Reasons might be the large area of the investigated region in the Northeast Atlantic Ocean during the

493 DRIVE campaign (25 ° latitude x 10 ° longitude) in contrast to this study along the Peruvian  
494 coast (12 ° latitude x 2 ° longitude). M91 observations therefore involve less variability of  
495 covered oceanic regimes of open ocean and coastal upwelling, VSLs concentrations and  
496 meteorological parameters, in particular of the MABL height, than the DRIVE observations.  
497 The Andes along South America lead to predominantly Southerly winds along the West coast  
498 line with minor continental influence, while the Mauritanian Upwelling is influenced by both,  
499 maritime and continental air masses. The latter can lead to strong surface inversions above  
500 the Mauritanian Upwelling and strongly suppressed mixing of surface air. Although our  
501 investigations revealed low MABL heights close to the Peruvian coast, the distinct surface  
502 inversions as observed above the Mauritanian Upwelling are not present in the available  
503 radiosonde data for this Peruvian Upwelling region. In addition, the relatively low sea-air  
504 fluxes of bromoform and dibromomethane, caused by moderate winds and small  
505 concentration gradients between the surface ocean and the surface atmosphere, as well as the  
506 short lifetime of methyl iodide lead to an insufficient enrichment of VSLs in the atmosphere.  
507 The observed air masses therefore contain VSLs mixing ratios which are predominantly  
508 advected. This is confirmed by our computed ADR (Section 3.4). The backward trajectories  
509 reveal air masses originating from the open ocean, which are transported along the coast for  
510 about 5 days until they reach the ship. In combination with the distinct trade inversion acting  
511 as strong barrier to the vertical mixing of trace gases, air-masses along the coast travel close  
512 to the surface where they can be enriched with local emissions before they are observed on-  
513 board. In addition, the in-situ observed oceanic emissions along the cruise track of R/V  
514 METEOR therefore cause small variations to the accumulated background mixing ratios of  
515 the advected air masses. This leads to lower correlation coefficients between the MABL  
516 height and the VSLs abundances compared to the Mauritanian Upwelling.

517 Although the oceanic emissions are already well mixed within days below the trade  
518 inversion, methyl iodide mixing ratios indicate a positive correlation with the trade inversion  
519 height, which is unexpected. The correlation coefficient might be artificial, as we observe  
520 elevated methyl iodide above the upwelling, where trade wind inversion heights are missing  
521 but can be assumed to be low (Riehl, 1954), which is also indicated by the correlation  
522 coefficients with SAT and SST. Nevertheless, this circumstance should be taken into account  
523 in future studies.

524 The contribution of oceanic emissions to the atmospheric mixing ratios in the MABL of the  
525 Peruvian upwelling reveals to be rather low in its more open ocean area under the given  
526 meteorological conditions. While the cruise track covered a representative area of the

527 Peruvian upwelling elevated oceanic VSLs emissions that could explain the generally high  
528 atmospheric VSLs were only observed for methyl iodide. Bromocarbon emissions would  
529 have to be two magnitudes larger to explain the observed VMR in the more open ocean  
530 regions and a magnitude larger in the direct coastal upwelling regions with low MABL  
531 heights. These observations of the brominated compounds need to include upwind advection  
532 of elevated sources from the South, and higher elevated coastal emissions not measured  
533 during the cruise, while dynamical fluctuations in emissions scenarios close to the cruise time  
534 and place may also have to be considered.

535 Uncertainties may result from the applied method, which accounts for a 400 m<sup>2</sup> box around a  
536 measurement point assuming steady state. The cruise track covered a significantly large area  
537 of the Peruvian Upwelling between 5° S and 16° S and higher elevated seas surface  
538 concentrations and emissions are not to be expected during these rather stable meteorological  
539 conditions. Additional uncertainties in our source-loss estimate may arise from deficiencies in  
540 the meteorological input fields from ERA-Interim reanalysis as well as from the air mass  
541 transport simulated by FLEXPART. Both could lead to either a shorter or longer residence  
542 time of the surface air masses within the MABL or below the trade inversion and thus  
543 influence the COL term. In particular very close to the coast, where the source-loss estimate  
544 could not be applied due to the trajectory analysis gaps (Section 2.5), the ODRs of the  
545 compounds might be different. Here potential high coastal emissions in combination with  
546 stable atmospheric stratification leading to slow vertical transport into the free troposphere,  
547 could significantly increase the oceanic contribution to the MABL and to the atmosphere  
548 below the trade inversion and explain the elevated atmospheric mixing ratios. In addition,  
549 different parameterizations for the wind-based transfer coefficient  $k_w$ , as discussed in  
550 Lennartz et al. (2015) and Fuhlbrügge et al (2015) in more detail, can impact the air-sea gas  
551 exchange and thus the ODRs. Applying the  $k_w$  parameterizations of Liss and Merlivat  
552 (1986) as well as Wanninkhof and McGillis (1999) lead both to mean ODRs in the MABL of  
553 0.02 (bromoform), 0.07 (dibromomethane) and 0.21 (methyl iodide) and below the trade  
554 inversion of 0.08 / 0.08 (bromoform), 0.25 / 0.26 (dibromomethane) and 0.69 / 0.75 (methyl  
555 iodide) and thus an even lower oceanic contribution to the atmosphere in this region. Further  
556 uncertainties may arise from variations of the MABL VSLs lifetimes and thus the chemical  
557 degradation of the compounds we use in this study. This would affect the computed  
558 advection (ADR) and not the oceanic contribution.

559 After the air masses are observed on R/V METEOR, the 10 day FLEXPART forward  
560 trajectories reveal a near-surface transport towards the equator (Figure 2~~Figure 1~~c-d). These

561 trajectories predominantly stay below 1 km altitude due to the horizontal extent of the trade  
562 inversion. The contribution of oceanic VSLs emissions from the Peruvian Upwelling to the  
563 free troposphere above this region is therefore strongly suppressed by the trade inversion  
564 (Figure 4 ~~Figure 3d~~). A contribution of oceanic emissions from the Peruvian Upwelling to the  
565 free troposphere is only achieved in the inner tropics after a transport time of 5 – 8 days,  
566 where the VSLs abundances are transported into higher altitudes. Since the lifetime of  
567 methyl iodide is only 4 days in the MABL a significant contribution of methyl iodide from  
568 the Peruvian upwelling to observations made by Yokouchi et al. (2008) at San Cristobal,  
569 Galapagos is not to be expected. However, it can partly explain the elevated IO observed  
570 above the Peruvian upwelling (Hepach et al., 2016, to be submitted; Schönhardt et al.,  
571 2008). ~~A contribution of oceanic emissions from the Peruvian Upwelling to the free~~  
572 ~~troposphere is only achieved in the ITCZ after a transport time of 5 – 8 days, where the VSLs~~  
573 ~~abundances are transported into higher altitudes. These transport paths may also explain the~~  
574 ~~elevated methyl iodide observed by Yokouchi et al. (2008) at San Cristobal, Galapagos and~~  
575 ~~the elevated IO of Schönhardt et al. (2008) and Dix et al. (2013) in the tropical East Pacific.~~  
576 The elevated mixing ratios of methyl iodide is further investigated by Hepach et al. (2015b).  
577 It has to be noted that the determined low contribution of oceanic emissions and boundary  
578 layer air to the free troposphere in this region is only representative for normal El Niño  
579 Southern Oscillation conditions as it was observed in December 2012  
580 ([http://www.cpc.ncep.noaa.gov/products/analysis\\_monitoring/enso\\_disc\\_nov2012/ensodisc.p](http://www.cpc.ncep.noaa.gov/products/analysis_monitoring/enso_disc_nov2012/ensodisc.pdf)  
581 [df](http://www.cpc.ncep.noaa.gov/products/analysis_monitoring/enso_disc_nov2012/ensodisc.pdf)). Since the Walker Circulation is reversed during El Niño, upwelling along the Peruvian  
582 coast is known to be suppressed and convective activity enhanced (Philander, 1989).

583

## 584 5. Summary

585 This study investigated the contribution of oceanic ~~VSLs~~ emissions to ~~their~~ VSLs  
586 abundances in the lowermost atmosphere as well as meteorological constraints on this  
587 contribution above both, ~~oceanic-coastal~~ upwelling ~~regions~~ and open ocean along the  
588 Peruvian coast during December 2012. Meteorological data were ~~measured-obtained~~ on R/V  
589 METEOR near the ocean surface and by radiosondes ~~launched~~ up to the stratosphere.  
590 Oceanic VSLs emissions along the cruise track were determined from air and ~~water samples~~  
591 ~~taken near the ocean surface~~ surface water data. ~~To investigate the transport of the observed~~  
592 ~~air masses, FLEXPART forward and backward trajectories were computed~~ The transport of  
593 air masses was determined with FLEXPART trajectories.

594 Oceanic upwelling was observed close to the Peruvian coast ~~by SST decreases to 15 °C~~  
595 ~~caused by the wind driven Ekman transport along the coast line with observed moderate wind~~  
596 ~~speeds of  $6.2 \pm 2.2 \text{ ms}^{-1}$ . The oceanic upwelling coincided with elevated relative humidity~~  
597 ~~including the formation of low level fog.~~ On average a low, stable MABL height of  $307 \pm$   
598  $177 \text{ m}$  was ~~determined from radiosonde launches and multiple linear regressions~~ encountered  
599 during the cruise, decreasing to on average 100 m above the upwelling. ~~A decrease of the~~  
600 ~~MABL height from the open ocean towards the coast was observed. The radiosonde launches~~  
601 ~~also revealed a~~ distinct trade inversion at  $1.1 \pm 0.3 \text{ km}$  height evolved as the dominant  
602 transport barrier for MABL air into the free troposphere during the cruise. ~~This study~~  
603 ~~concentrates on the three~~ The halogenated VSLs: bromoform, ~~and~~ dibromomethane ~~and~~  
604 methyl iodide. ~~Except for methyl iodide, showed low oceanic emissions were low with of 130~~  
605  $117 \pm 554\text{--}492 \text{ pmol m}^{-2} \text{ hr}^{-1}$  for bromoform, ~~and~~  $273\text{--}245 \pm 334\text{--}299 \text{ pmol m}^{-2} \text{ hr}^{-1}$  for  
606 dibromomethane, ~~and while methyl iodide emissions were elevated with~~  $954\text{--}856 \pm 697\text{--}623$   
607  $\text{pmol m}^{-2} \text{ hr}^{-1}$  ~~for methyl iodide. Despite the low oceanic emissions, t~~ The atmospheric mixing  
608 ratios of the compounds were elevated with  $2.9 \pm 0.7 \text{ ppt}$  (bromoform),  $1.3 \pm 0.3 \text{ ppt}$   
609 (dibromomethane) and  $1.5 \pm 0.5 \text{ ppt}$  (methyl iodide). ~~According to our FLEXPART ERA-~~  
610 ~~Interim trajectory calculations, the average residence time of surface air masses in the~~  
611 ~~observed MABL was 7 hours. Once these air masses left the MABL, they were suppressed in~~  
612 ~~their vertical movement by the trade inversion, which was reflected by an average residence~~  
613 ~~time of 41 hours below the trade inversion. This additional distinct inversion layer evolved as~~  
614 ~~the dominant transport barrier for MABL air into the free troposphere and led to an~~  
615 ~~accumulation of air masses and the VSLs abundances therein observed during the cruise.~~  
616 ~~With a simple source loss estimate we computed the ratio between the contribution of~~  
617 ~~oceanic emissions and advection to the loss of air into the free troposphere.~~ The oceanic  
618 emissions along the cruise track explained on average only ~~12 %~~ 3 % (-8 to 33 %) ~~for~~ of  
619 bromoform, ~~and 37 %~~ 10 % (-5 to 45 %) ~~for~~ of dibromomethane, ~~but and~~ 103-28 % (3 to  
620 80 %) ~~for~~ of methyl iodide ~~of the observed VSLs abundances. Considering the chemical~~  
621 ~~degradation of the compounds during the residence time of the trajectories below the trade~~  
622 ~~inversion in the MABL. Thus, the expected significant contribution of local oceanic VSLs~~  
623 ~~emissions from the Peruvian upwelling to the overlying atmosphere was not captured during~~  
624 ~~the time and location of the cruise., a residual advective transport of 104 % (bromoform), 68~~  
625 ~~% (dibromomethane) and 69 % (methyl iodide) was necessary to explain the observed~~  
626 ~~atmospheric VSLs mixing ratios.~~ The elevated atmospheric VSLs ~~observed on R/V~~  
627 ~~METEOR~~ were mixing ratios above the Peruvian upwelling therefore appear largely

628 | advected and enriched along the Peruvian coast before reaching the ship. –Additional  
629 | potential source regions must exist closer to the coast and also further South of the cruise  
630 | track along the coast line. Nevertheless, significant correlation ~~coefficients~~ between the  
631 | MABL height and marine atmospheric abundances of bromoform ( $R = -0.55$ ),  
632 | dibromomethane ( $R = -0.61$ ), respectively methyl iodide ( $R = -0.45$ ) the VSLs reveal an  
633 | impact of the low-oceanic emissions on the atmospheric VSLs abundances. ~~The lower~~  
634 | ~~correlation between the MABL height and the atmospheric VSLs in this oceanic region~~  
635 | ~~compared to the Mauritanian Upwelling was identified to be caused by less variability of~~  
636 | ~~oceanic regimes and more stable atmospheric regimes during this cruise mixing ratio~~  
637 | ~~variations.~~

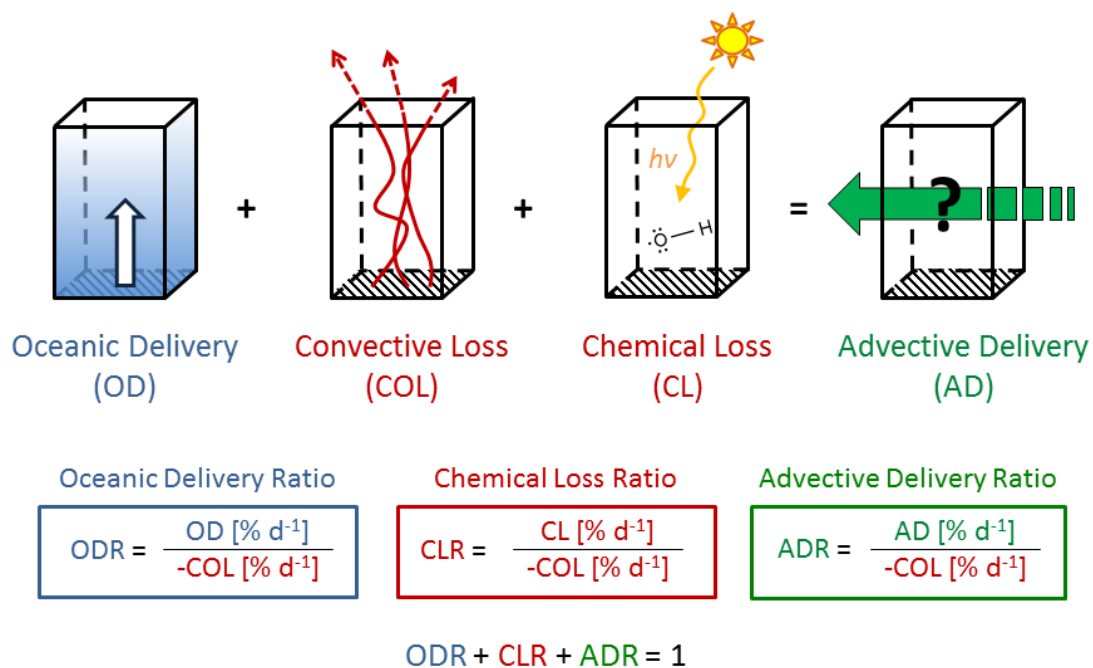
638 | Our study confirms that MABL height and ~~characteristics stability is~~ are generally related  
639 | with atmospheric VSLs abundances above oceanic upwelling regions. Additionally, a  
640 | widespread trade inversion can lead to a near-surface accumulation of the VSLs ~~which~~  
641 | ~~impacts oceanic emissions and therefore feedback on VSLs concentrations in the lower~~  
642 | ~~atmosphere~~ ~~The~~ and thus also impact oceanic emissions. Despite the observed elevated  
643 | atmospheric concentrations during the cruise, a significant contribution of oceanic emissions  
644 | to the atmosphere, in particular of the bromocarbons bromoform and dibromomethane, was  
645 | not identified in the observed area during the time of the cruise. Further studies are necessary  
646 | to clearly uncover the source regions of the elevated atmospheric VSLs in the Peruvian  
647 | upwelling. Also the ~~The~~ double transport barrier phenomena should be investigated in future  
648 | studies of other oceanic upwelling regions as well.

649

650       **Acknowledgements**

651       This study was supported by the BMBF grant SOPRAN II FKZ 03F0611A. We acknowledge  
652       the authorities of Peru for the permissions to work in their territorial waters. We thank the  
653       European Centre for medium range weather forecast (ECMWF) for the provision of ERA-  
654       Interim reanalysis data and the Lagrangian particle dispersion model FLEXPART used in this  
655       publication. We also like to thank the captain and crew of R/V METEOR, and the Deutscher  
656       Wetterdienst (DWD) for the support.

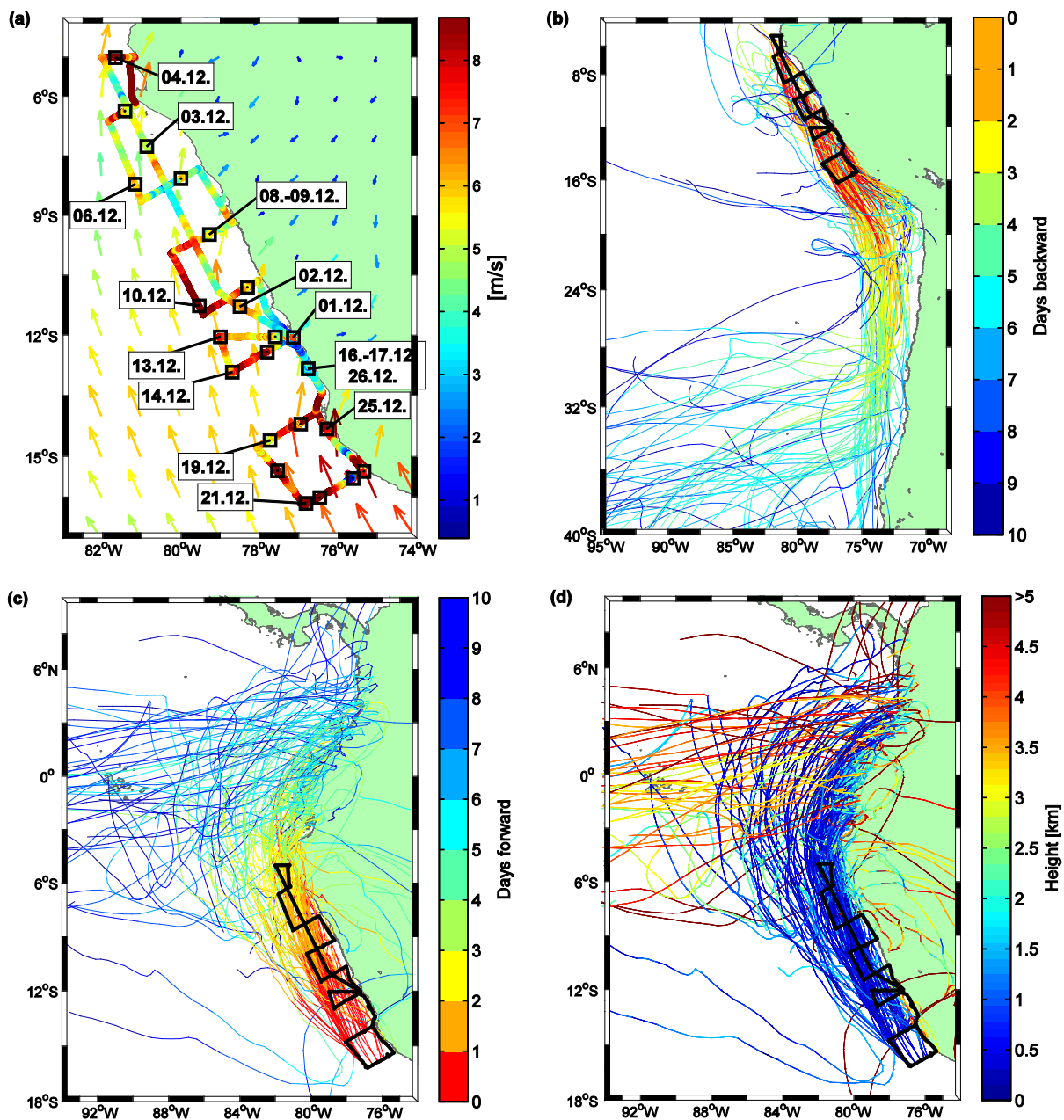
657



659

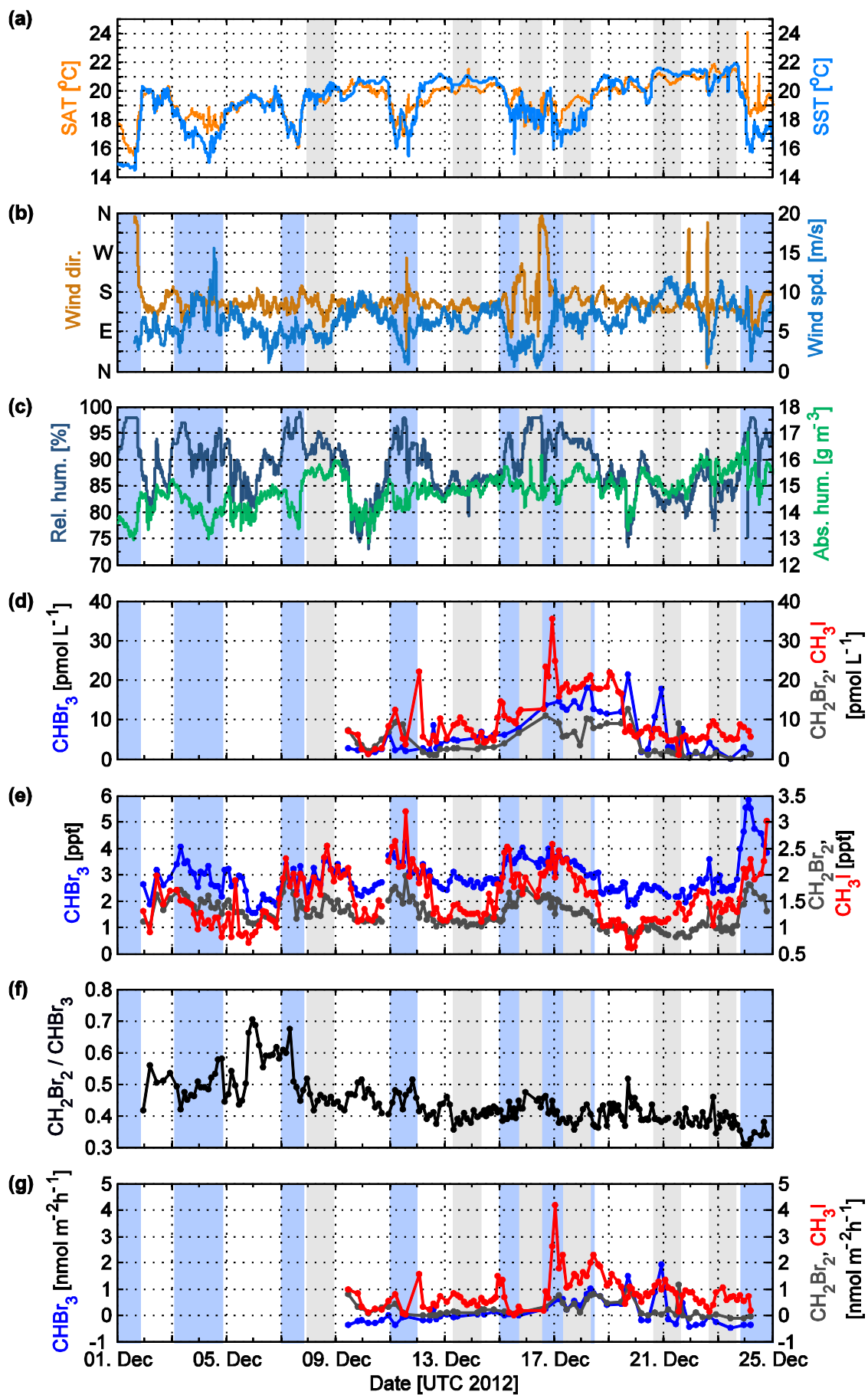
660 Figure 1: Schematic summary of the components of the applied mass-balance concept from  
 661 Fuhlbrügge et al. (2015): Oceanic Delivery (OD), the Convective Loss (COL), the Chemical  
 662 Loss (CL), the Advective Delivery (AD), the Oceanic Delivery Ratio (ODR), the Chemical  
 663 Loss Ratio (CLR) and the Advective Delivery Ratio (ADR). The shaded area reflects an area  
 664 of 400 m<sup>2</sup>.

665



666

667 Figure 2a-d: (a) 10 minute mean of wind speed observed on R/V METEOR displayed along  
 668 the cruise track; monthly mean (December 2012) of 10 m wind speed and direction from  
 669 ERA-Interim displayed as arrows. (b) Extract from 10-day FLEXPART backward trajectories  
 670 coloured according to the time until they reach the specific ship position on the cruise track of  
 671 R/V METEOR (black). (c) Extract from 10-day FLEXPART forward trajectories coloured  
 672 according to the time since they were released. (d) same as c) coloured according to the  
 673 height (km) of the trajectories.

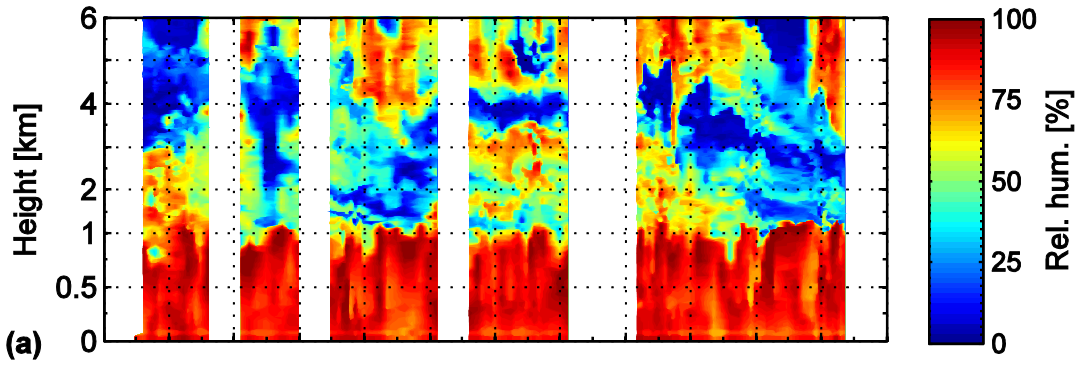


675 Figure 3a-e: Observations during December 1 – 25, 2012 on R/V METEOR. Diurnal stations  
676 are indicated by grey background shades. (a) 10 minute mean of the SAT (orange) and the  
677 SST (blue) in °C. According to SST decrease, upwelling regions are marked with a light blue  
678 | background shade in ~~Figure 3~~ ~~Figure 2~~ b-e. (b) 10 minute mean of wind direction in cardinal  
679 directions (ocher) and wind speed in m/s (blue). (c) 10 minute mean of relative humidity in %  
680 (dark blue) and absolute humidity in  $\text{gm}^{-3}$  (green). (d) Oceanic surface concentrations of  
681 bromoform ( $\text{CHBr}_3$ , blue), dibromomethane ( $\text{CH}_2\text{Br}_2$ , dark grey) and methyl iodide ( $\text{CH}_3\text{I}$ ,  
682 red) in  $\text{pmol L}^{-1}$ . (e) Atmospheric mixing ratios of bromoform, dibromomethane and methyl  
683 iodide in ppt. (f) Concentration ratio of dibromomethane and bromoform. (g) Sea-air flux for  
684 bromoform, dibromomethane and methyl iodide in  $\text{pmol m}^{-2} \text{h}^{-1}$ .

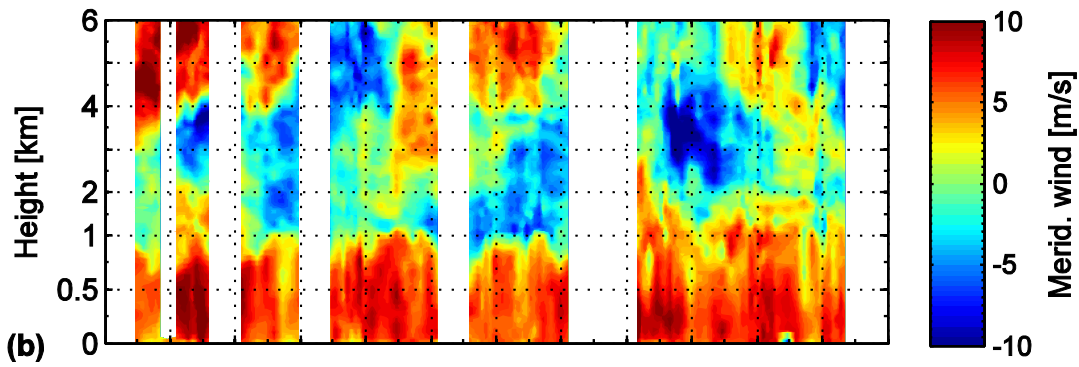
685 Table 1: Oceanic concentrations, atmospheric mixing ratios and sea-air fluxes of bromoform  
 686 ( $\text{CHBr}_3$ ), dibromomethane ( $\text{CH}_2\text{Br}_2$ ), the concentration ratio of bromoform and  
 687 dibromomethane and methyl iodide ( $\text{CH}_3\text{I}$ ) observed during the cruise. Values are given in  
 688 mean  $\pm 1\sigma$  [range].

	$\text{CHBr}_3$	$\text{CH}_2\text{Br}_2$	$\text{CH}_2\text{Br}_2 / \text{CHBr}_3$	$\text{CH}_3\text{I}$
Oceanic concentration [ $\text{pmol L}^{-1}$ ]	$6.6 \pm 5.5$ [0.2 – 21.5]	$4.3 \pm 3.4$ [0.2 – 12.7]	$0.9 \pm 0.8$ [0.1 – 4.2]	$9.8 \pm 6.3$ [1.1 – 35.4]
Atmospheric mixing ratio [ppt]	$2.9 \pm 0.7$ [1.5 – 5.9]	$1.3 \pm 0.3$ [0.8 – 2.0]	$0.4 \pm 0.1$ [0.3 – 0.7]	$1.5 \pm 0.5$ [0.6 – 3.2]
Sea-air flux [ $\text{pmol m}^{-2} \text{ hr}^{-1}$ ]	<del>130</del> 117 $\pm$ 554492 [-550477 – 22011916]	<del>273</del> 245 $\pm$ 334299 [-128112 – 13211169]	$0.4 \pm 8.6$ [-24.5 – 48.9]	<del>954</del> 856 $\pm$ 697623 [2118 - 46874179]

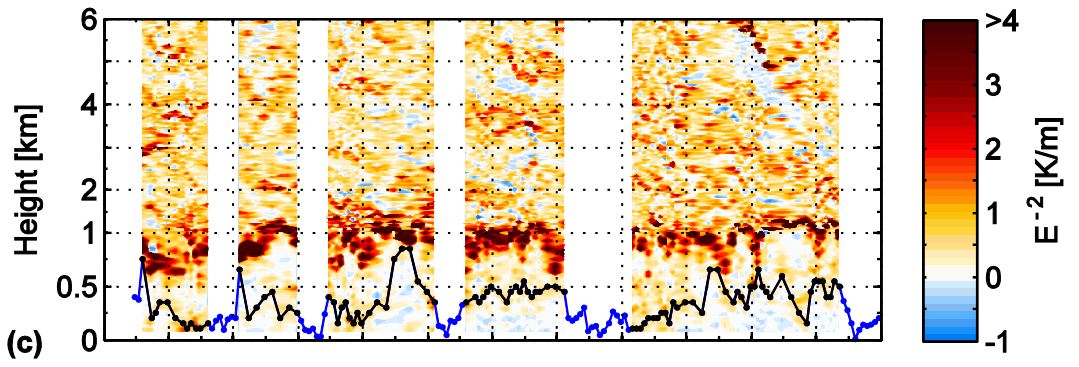
689



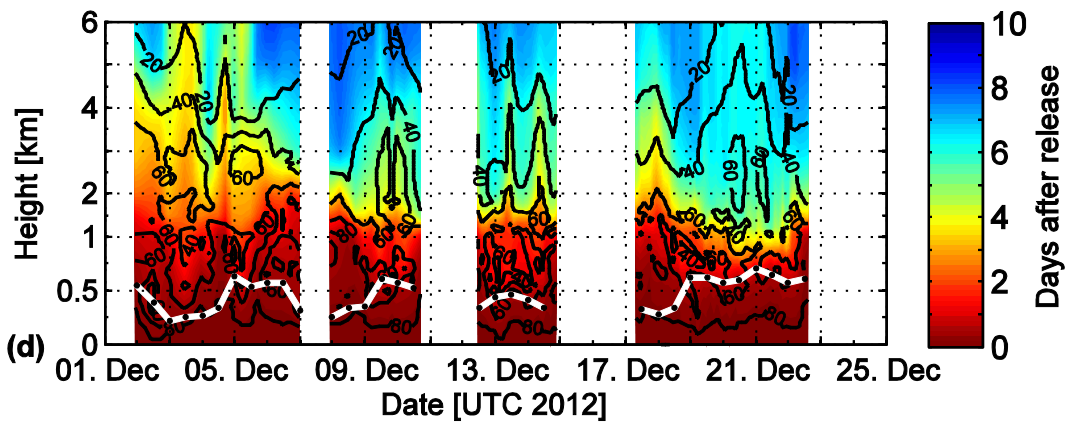
690



691



692



693

694 Figure 4: (a-c) Radiosonde observations of the lower 6 km of the atmosphere between  
695 December 2 and 24, 2012 on R/V Meteor. Shown are (a) the relative humidity in %, (b) the  
696 meridional wind in m/s and (c) the gradient of the virtual potential temperature in  $E^{-2}$  K/m in  
697 combination with the determined MABL height (black) and the complimented MABL height  
698 above the oceanic upwelling from the multiple linear regressions (blue). (d) Distribution of  
699 10-day FLEXPART forward trajectories. The black contour lines give the amount of  
700 trajectories in percentage that reach a specific altitude within the 10 days. The elapsed time in  
701 days until these trajectories reach this height is reflected by the colour shading. The white line  
702 shows the ERA-Interim MABL height at the ship position. Trajectory analyses gaps close to  
703 the coast are whitened (Section 2.5). The y-axes are non-linear.

704 Table 2: Mean  $\pm 1\sigma$  of Oceanic Delivery (OD), Advective Delivery (AD), Chemical Loss  
705 (CL), CONvective Loss (COL), Oceanic Delivery Ratio (ODR), Advective Delivery Ratio  
706 (ADR) and Chemical Loss Ratio (CLR) of bromoform ( $\text{CHBr}_3$ ), dibromomethane ( $\text{CH}_2\text{Br}_2$ )  
707 and methyl iodide ( $\text{CH}_3\text{I}$ ). Parameters have been computed for a box with the vertical  
708 extension of the MABL height (MABLH) and a mean trade inversion height of 1.1 km (TIH).

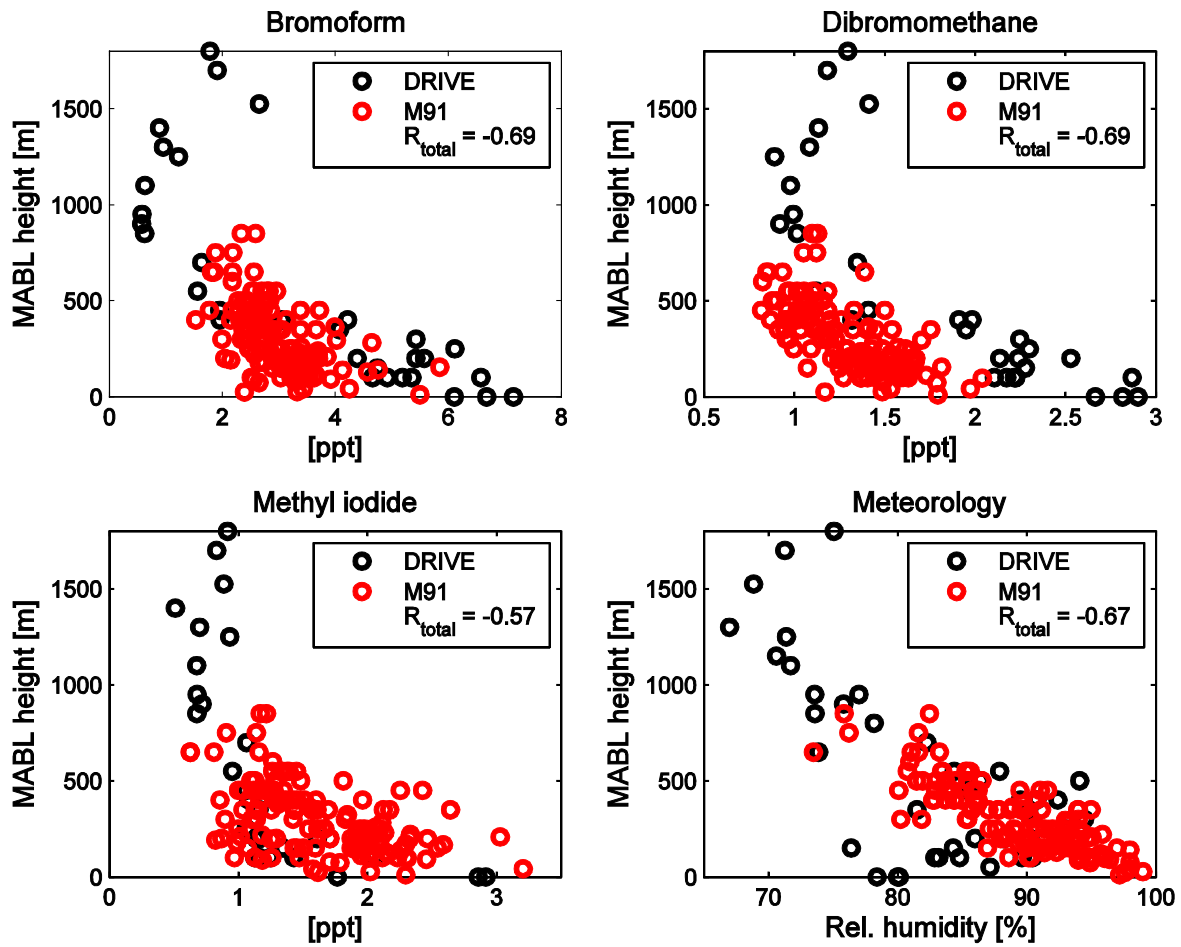
		OD [% d <sup>-1</sup> ]	AD [% d <sup>-1</sup> ]	CL [% d <sup>-1</sup> ]	COL [% d <sup>-1</sup> ]	ODR	ADR	CLR
$\text{CHBr}_3$	MABLH	<del>109.21</del> $\pm$ <del>3128.20</del>	<del>347349.50</del> $\pm$ <del>114113.34</del>	<del>-67.61</del>	- <del>341351.70</del> $\pm$ <del>118109.24</del>	0.03 $\pm$ 0.0908	0.99 $\pm$ 0.0908	-0.02 $\pm$ 0.01
	TIH	<del>43.49</del> $\pm$ <del>1312.60</del>	<del>5253.32</del> $\pm$ <del>2423.32</del>	<del>-67.61</del>	<del>-5850.50</del> $\pm$ <del>2718.4</del>	0.1211 $\pm$ 0.45	<del>1.0406</del> $\pm$ 0.4439	- 0.1617 $\pm$ 0.07
$\text{CH}_2\text{Br}_2$	MABLH	<del>3632.01</del> $\pm$ <del>4338.57</del>	<del>317320.01</del> $\pm$ <del>117115.26</del>	<del>-1.82</del>	- <del>341351.70</del> $\pm$ <del>118109.24</del>	0.1110 $\pm$ 0.1211	0.90 $\pm$ 0.1211	- 0.0100 $\pm$ 0.00
	TIH	<del>1513.38</del> $\pm$ <del>1816.65</del>	<del>3637.54</del> $\pm$ <del>2725.49</del>	<del>-1.82</del>	<del>-5850.50</del> $\pm$ <del>2718.4</del>	0.3733 $\pm$ 0.6154	0.67 $\pm$ 0.6154	- 0.0403 $\pm$ 0.0201
$\text{CH}_3\text{I}$	MABLH	<del>8896.29</del> $\pm$ <del>5348.71</del>	<del>276286.21</del> $\pm$ <del>122119.67</del>	- <del>3024.70</del>	- <del>341351.70</del> $\pm$ <del>118109.24</del>	0.3128 $\pm$ 0.1817	0.7980 $\pm$ 0.1716	- 0.1008 $\pm$ 0.034
	TIH	<del>4136.18</del> $\pm$ <del>2320.05</del>	<del>3937.52</del> $\pm$ <del>3432.21</del>	- <del>3024.70</del>	<del>-5850.50</del> $\pm$ <del>2718.4</del>	<del>10.0392</del> $\pm$ 0.7869	0.6964 $\pm$ 0.6655	- 0.7256 $\pm$ 0.3124

709

710 Table 3: Spearman correlation coefficients (R) of meteorological parameters, MABL height  
 711 and trade inversion height correlated with atmospheric bromoform (CHBr<sub>3</sub>), dibromomethane  
 712 (CH<sub>2</sub>Br<sub>2</sub>) and methyl iodide (CH<sub>3</sub>I). MABL height\* is the determined MABL height from the  
 713 radiosonde launches, complimented by the regressed MABL height (Section 3.3). Bold  
 714 coefficients have a p-value of < 0.05.

	MABL height	MABL height*	Trade inversion	CHBr <sub>3</sub>	CH <sub>2</sub> Br <sub>2</sub>	CH <sub>3</sub> I
Wind speed	<b>0.35</b>	<b>0.44</b>	-0.06	<b>-0.38</b>	<b>-0.53</b>	<b>-0.33</b>
SAT	<b>0.65</b>	<b>0.79</b>	<b>0.24</b>	<b>-0.50</b>	<b>-0.78</b>	<b>-0.37</b>
SST	<b>0.66</b>	<b>0.80</b>	<b>0.23</b>	<b>-0.57</b>	<b>-0.81</b>	<b>-0.42</b>
SAT – SST	<b>-0.39</b>	<b>-0.47</b>	-0.11	<b>0.38</b>	<b>0.48</b>	<b>0.30</b>
Rel. humidity	<b>-0.77</b>	<b>-0.81</b>	-0.06	<b>0.74</b>	<b>0.77</b>	<b>0.67</b>
MABL height*	-	-	0.08	<b>-0.55</b>	<b>-0.61</b>	<b>-0.45</b>
CHBr <sub>3</sub>	<b>-0.55</b>	<b>-0.60</b>	-0.03	-	<b>0.79</b>	<b>0.79</b>
CH <sub>2</sub> Br <sub>2</sub>	<b>-0.61</b>	<b>-0.72</b>	-0.02	<b>0.79</b>	-	<b>0.66</b>
CH <sub>3</sub> I	<b>-0.45</b>	<b>-0.50</b>	<b>0.30</b>	<b>0.79</b>	<b>0.66</b>	-

715



716

717 Figure 5: Scatter plots of atmospheric mixing ratios of bromoform, dibromomethane, methyl  
 718 iodide and relative humidity vs. MABL height. ~~Blue-Black~~ circles reflect observations from  
 719 the ~~DRIVE~~ campaign in the Mauritanian Upwelling (Fuhlbrügge et al., 2013) and ~~black-red~~  
 720 circles from this study (M91).  $R_{total}$  gives the Spearman correlation coefficients for both data  
 721 sets together.

722

723 **References**

- 724 Butler, J., King, D., Lobert, J., Montzka, S., Yvon-Lewis, S., Hall, B., Warwick, N., Mondeel, D., Aydin,  
725 M., and Elkins, J.: Oceanic distributions and emissions of short-lived halocarbons, *Global*  
726 *Biogeochemical Cycles*, 21, 10.1029/2006GB002732, 2007.
- 727 Carpenter, L., Liss, P., and Penkett, S.: Marine organohalogens in the atmosphere over the Atlantic  
728 and Southern Oceans, *Journal of Geophysical Research-Atmospheres*, 108, 10.1029/2002JD002769,  
729 2003.
- 730 Carpenter, L., Jones, C., Dunk, R., Hornsby, K., and Woeltjen, J.: Air-sea fluxes of biogenic bromine  
731 from the tropical and North Atlantic Ocean, *Atmospheric Chemistry and Physics*, 9, 1805-1816, 2009.
- 732 Carpenter, L., Fleming, Z., Read, K., Lee, J., Moller, S., Hopkins, J., Purvis, R., Lewis, A., Muller, K.,  
733 Heinold, B., Herrmann, H., Fomba, K., van Pinxteren, D., Muller, C., Tegen, I., Wiedensohler, A.,  
734 Muller, T., Niedermeier, N., Achterberg, E., Patey, M., Kozlova, E., Heimann, M., Heard, D., Plane, J.,  
735 Mahajan, A., Oetjen, H., Ingham, T., Stone, D., Whalley, L., Evans, M., Pilling, M., Leigh, R., Monks, P.,  
736 Karunaharan, A., Vaughan, S., Arnold, S., Tschirner, J., Pohler, D., Friess, U., Holla, R., Mendes, L.,  
737 Lopez, H., Faria, B., Manning, A., and Wallace, D.: Seasonal characteristics of tropical marine  
738 boundary layer air measured at the Cape Verde Atmospheric Observatory, *Journal of Atmospheric*  
739 *Chemistry*, 67, 87-140, 10.1007/s10874-011-9206-1, 2010.
- 740 Carpenter, L. J., Reimann, S., Burkholder, J. B., Clerbaux, C., Hall, B. D., Hossaini, R., Laube, J. C., and  
741 Yvon-Lewis, S. A.: Update on Ozone-Depleting Substances (ODSs) and Other Gases of Interest to the  
742 Montreal Protocol, in: *Scientific Assessment of Ozone Depletion: 2014*, edited by: Engel, A., and  
743 Montzka, S. A., World Meteorological Organization, Geneva, 2014.
- 744 Codispoti, L. A., Dugdale, R. C., and Minas, H. J.: A comparison of the nutrient regimes off Northwest  
745 Africa, Peru and Baja California, *Rapport et Procés-verbaux des réunions. Conseil permanent*  
746 *International pour l'Exploration de la Mer*, 184-201 pp., 1982.
- 747 Dix, B., Baidara, S., Bresch, J., Hall, S., Schmidt, K., Wang, S., and Volkamer, R.: Detection of iodine  
748 monoxide in the tropical free troposphere, *Proceedings of the National Academy of Sciences of the*  
749 *United States of America*, 110, 2035-2040, 10.1073/pnas.1212386110, 2013.
- 750 Forster, C., Stohl, A., and Seibert, P.: Parameterization of convective transport in a Lagrangian  
751 particle dispersion model and its evaluation, *Journal of Applied Meteorology and Climatology*, 46,  
752 403-422, 10.1175/JAM2470.1, 2007.
- 753 Fuhlbrügge, S., Krüger, K., Quack, B., Atlas, E., Hepach, H., and Ziska, F.: Impact of the marine  
754 atmospheric boundary layer conditions on VSLs abundances in the eastern tropical and subtropical  
755 North Atlantic Ocean, *Atmospheric Chemistry and Physics*, 13, 6345-6357, 10.5194/acp-13-6345-  
756 2013, 2013.
- 757 Fuhlbrügge, S., Quack, B., Tegtmeier, S., Atlas, E., Hepach, H., Shi, Q., Raimund, S., and Krüger, K.:  
758 The contribution of oceanic very short lived halocarbons to marine and free troposphere air over the  
759 tropical West Pacific, *Atmos. Chem. Phys. Discuss.*, 15, 17887-17943, 10.5194/acpd-15-17887-2015,  
760 2015.
- 761 Garreaud, R., and Munoz, R.: The low-level jet off the west coast of subtropical South America:  
762 Structure and variability, *Monthly Weather Review*, 133, 2246-2261, 10.1175/MWR2972.1, 2005.
- 763 Gómez Martin, J., Mahajan, A., Hay, T., Prados-Roman, C., Ordonez, C., MacDonald, S., Plane, J.,  
764 Sorribas, M., Gil, M., Mora, J., Reyes, M., Oram, D., Leedham, E., and Saiz-Lopez, A.: Iodine chemistry  
765 in the eastern Pacific marine boundary layer, *Journal of Geophysical Research-Atmospheres*, 118,  
766 887-904, 10.1002/jgrd.50132, 2013.
- 767 Hepach, H., Quack, B., Ziska, F., Fuhlbrügge, S., Atlas, E., Krüger, K., Peeken, I., and Wallace, D. W. R.:  
768 Drivers of diel and regional variations of halocarbon emissions from the tropical North East Atlantic,  
769 *Atmos. Chem. Phys.*, 14, 10.5194/acp-14-1255-2014, 2014.
- 770 Hepach, H., Quack, B., Raimund, S., Fischer, T., Atlas, E. L., and Bracher, A.: Halocarbon emissions  
771 and sources in the equatorial Atlantic Cold Tongue, *Biogeosciences Discuss.*, 12, 5559-5608,  
772 10.5194/bgd-12-5559-2015, 2015a.

773 Hepach, H., Quack, B., Tegtmeier, S., Engel, A., Bracher, A., Fuhlbrügge, S., Raimund, S., Lampel, J., L.,  
774 G., and Krüger, K.: Contributions of biogenic halogenated compounds from the Peruvian upwelling  
775 to the tropical troposphere, to be submitted, 2015b.

776 Hepach, H., Quack, B., Tegtmeier, S., Engel, A., Bracher, A., Fuhlbrügge, S., L., G., Atlas, E., Lampel, J.,  
777 Frieß, U., and Krüger, K.: Biogenic halocarbons from the Peruvian upwelling region as tropospheric  
778 halogen source, to be submitted, 2016.

779 Hossaini, R., Chipperfield, M., Monge-Sanz, B., Richards, N., Atlas, E., and Blake, D.: Bromoform and  
780 dibromomethane in the tropics: a 3-D model study of chemistry and transport, *Atmospheric*  
781 *Chemistry and Physics*, 10, 719-735, 10.5194/acp-10-719-2010, 2010.

782 Höflich, O.: The meteorological effects of cold upwelling water areas, *Geoforum*, 3, 35-46,  
783 10.1016/0016-7185(72)90084-X, 1972.

784 Lennartz, S. T., Krysztofiak, G., Marandino, C. A., Sinnhuber, B. M., Tegtmeier, S., Ziska, F., Hossaini,  
785 R., Krüger, K., Montzka, S. A., Atlas, E., Oram, D. E., Keber, T., Bönisch, H., and Quack, B.: Modelling  
786 marine emissions and atmospheric distributions of halocarbons and dimethyl sulfide: the influence  
787 of prescribed water concentration vs. prescribed emissions, *Atmos. Chem. Phys.*, 15, 11753-11772,  
788 10.5194/acp-15-11753-2015, 2015.

789 Liss, P. S., and Merlivat, L.: Air-Sea Gas Exchange Rates: Introduction and Synthesis, in: *The Role of*  
790 *Air-Sea Exchange in Geochemical Cycling*, edited by: Buat-Menard, P., Reidel, D., and Norwell, M.,  
791 Springer Netherlands, 113-127, 1986.

792 Liu, Y., Yvon-Lewis, S., Thornton, D., Butler, J., Bianchi, T., Campbell, L., Hu, L., and Smith, R.: Spatial  
793 and temporal distributions of bromoform and dibromomethane in the Atlantic Ocean and their  
794 relationship with photosynthetic biomass, *Journal of Geophysical Research-Oceans*, 118, 3950-3965,  
795 10.1002/jgrc.20299, 2013.

796 Mahajan, A., Martin, J., Hay, T., Royer, S., Yvon-Lewis, S., Liu, Y., Hu, L., Prados-Roman, C., Ordonez,  
797 C., Plane, J., and Saiz-Lopez, A.: Latitudinal distribution of reactive iodine in the Eastern Pacific and its  
798 link to open ocean sources, *Atmospheric Chemistry and Physics*, 12, 11609-11617, 10.5194/acp-12-  
799 11609-2012, 2012.

800 McGivern, W., Sorkhabi, O., Suits, A., Derecskei-Kovacs, A., and North, S.: Primary and secondary  
801 processes in the photodissociation of CHBr<sub>3</sub>, *Journal of Physical Chemistry a*, 104, 10085-10091,  
802 10.1021/jp0005017, 2000.

803 Nightingale, P., Malin, G., Law, C., Watson, A., Liss, P., Liddicoat, M., Boutin, J., and Upstill-Goddard,  
804 R.: In situ evaluation of air-sea gas exchange parameterizations using novel conservative and volatile  
805 tracers, *Global Biogeochemical Cycles*, 14, 373-387, 10.1029/1999GB900091, 2000.

806 O'Brien, L., Harris, N., Robinson, A., Gostlow, B., Warwick, N., Yang, X., and Pyle, J.: Bromocarbons in  
807 the tropical marine boundary layer at the Cape Verde Observatory - measurements and modelling,  
808 *Atmospheric Chemistry and Physics*, 9, 9083-9099, 10.5194/acp-9-9083-2009, 2009.

809 Philander, G.: El-Nino and La-Nina, *American Scientist*, 77, 451-459, 1989.

810 Quack, B., Atlas, E., Petrick, G., Stroud, V., Schauffler, S., and Wallace, D.: Oceanic bromoform  
811 sources for the tropical atmosphere, *Geophysical Research Letters*, 31, 10.1029/2004GL020597,  
812 2004.

813 Quack, B., Atlas, E., Petrick, G., and Wallace, D.: Bromoform and dibromomethane above the  
814 Mauritanian upwelling: Atmospheric distributions and oceanic emissions, *Journal of Geophysical*  
815 *Research-Atmospheres*, 112, 10.1029/2006JD007614, 2007.

816 Raimund, S., Quack, B., Bozec, Y., Vernet, M., Rossi, V., Garçon, V., Morel, Y., and Morin, P.: Sources  
817 of short-lived bromocarbons in the Iberian upwelling system, *Biogeosciences*, 8, 1551-1564,  
818 10.5194/bg-8-1551-2011, 2011.

819 Rasmussen, R., Khalil, M., Gunawardena, R., and Hoyt, S.: Atmospheric methyl-iodide (CH<sub>3</sub>I), *Journal*  
820 *of Geophysical Research-Oceans and Atmospheres*, 87, 3086-3090, 10.1029/JC087iC04p03086,  
821 1982.

822 Riehl, H.: *Tropical meteorology*, McGraw-Hill, New York-London, 1954.

823 Riehl, H.: *Climate and Weather in the Tropics*, Academic Press, London, 1979.

824 Saiz-Lopez, A., Lamarque, J., Kinnison, D., Tilmes, S., Ordonez, C., Orlando, J., Conley, A., Plane, J.,  
825 Mahajan, A., Santos, G., Atlas, E., Blake, D., Sander, S., Schauffler, S., Thompson, A., and Brasseur, G.:  
826 Estimating the climate significance of halogen-driven ozone loss in the tropical marine troposphere,  
827 *Atmospheric Chemistry and Physics*, 12, 3939-3949, 10.5194/acp-12-3939-2012, 2012.  
828 Saiz-Lopez, A., and von Glasow, R.: Reactive halogen chemistry in the troposphere, *Chemical Society*  
829 *Reviews*, 41, 6448-6472, 10.1039/c2cs35208g, 2012.  
830 Schauffler, S., Atlas, E., Blake, D., Flocke, F., Lueb, R., Lee-Taylor, J., Stroud, V., and Travnicek, W.:  
831 Distributions of brominated organic compounds in the troposphere and lower stratosphere, *Journal*  
832 *of Geophysical Research-Atmospheres*, 104, 21513-21535, 10.1029/1999JD900197, 1999.  
833 Schönhardt, A., Richter, A., Wittrock, F., Kirk, H., Oetjen, H., Roscoe, H., and Burrows, J.:  
834 Observations of iodine monoxide columns from satellite, *Atmospheric Chemistry and Physics*, 8, 637-  
835 653, 10.5194/acp-8-637-2008, 2008.  
836 Seibert, P., Beyrich, F., Gryning, S., Joffre, S., Rasmussen, A., and Tercier, P.: Review and  
837 intercomparison of operational methods for the determination of the mixing height, *Atmospheric*  
838 *Environment*, 34, 1001-1027, 10.1016/S1352-2310(99)00349-0, 2000.  
839 Simpson, W., Brown, S., Saiz-Lopez, A., Thornton, J., and von Glasow, R.: Tropospheric Halogen  
840 Chemistry: Sources, Cycling, and Impacts, *Chemical Reviews Article ASAP*, 4035-4062,  
841 10.1021/cr5006638, 2015.  
842 Stohl, A., Hittenberger, M., and Wotawa, G.: Validation of the Lagrangian particle dispersion model  
843 FLEXPART against large-scale tracer experiment data, *Atmospheric Environment*, 32, 4245-4264,  
844 10.1016/S1352-2310(98)00184-8, 1998.  
845 Stohl, A., and Thomson, D.: A density correction for Lagrangian particle dispersion models,  
846 *Boundary-Layer Meteorology*, 90, 155-167, 10.1023/A:1001741110696, 1999.  
847 Stohl, A., and Trickl, T.: A textbook example of long-range transport: Simultaneous observation of  
848 ozone maxima of stratospheric and North American origin in the free troposphere over Europe,  
849 *Journal of Geophysical Research-Atmospheres*, 104, 30445-30462, 10.1029/1999JD900803, 1999.  
850 Stohl, A., Forster, C., Frank, A., Seibert, P., and Wotawa, G.: Technical note: The Lagrangian particle  
851 dispersion model FLEXPART version 6.2, *Atmospheric Chemistry and Physics*, 5, 2461-2474, 2005.  
852 Stull, R.: *An Introduction to Boundary Layer Meteorology*, Kluwer Academic Publishers, Dordrecht,  
853 1988.  
854 Wanninkhof, R., and McGillis, W.: A cubic relationship between air-sea CO<sub>2</sub> exchange and wind  
855 speed, *Geophysical Research Letters*, 26, 1889-1892, 10.1029/1999GL900363, 1999.  
856 Yokouchi, Y., Li, H., Machida, T., Aoki, S., and Akimoto, H.: Isoprene in the marine boundary layer  
857 (Southeast Asian Sea, eastern Indian Ocean, and Southern Ocean): Comparison with dimethyl sulfide  
858 and bromoform, *Journal of Geophysical Research-Atmospheres*, 104, 8067-8076,  
859 10.1029/1998JD100013, 1999.  
860 Yokouchi, Y., Hasebe, F., Fujiwara, M., Takashima, H., Shiotani, M., Nishi, N., Kanaya, Y., Hashimoto,  
861 S., Fraser, P., Toom-Saunty, D., Mukai, H., and Nojiri, Y.: Correlations and emission ratios among  
862 bromoform, dibromochloromethane, and dibromomethane in the atmosphere, *Journal of*  
863 *Geophysical Research-Atmospheres*, 110, 10.1029/2005JD006303, 2005.  
864 Yokouchi, Y., Osada, K., Wada, M., Hasebe, F., Agama, M., Murakami, R., Mukai, H., Nojiri, Y.,  
865 Inuzuka, Y., Toom-Saunty, D., and Fraser, P.: Global distribution and seasonal concentration change  
866 of methyl iodide in the atmosphere, *Journal of Geophysical Research-Atmospheres*, 113,  
867 10.1029/2008JD009861, 2008.

868